

## Highlights

### **Synthesising Activity Participations and Scheduling with Deep Generative Machine Learning**

Fred Shone, Dr Tim Hillel

- We contribute a novel approach to synthesising human activity schedules using deep generative modelling. Specifically, we demonstrate the rapid synthesis of large, realistic samples of human activity schedules using Variational Auto-Encoders.
- We propose a novel activity schedule encoding, using a continuous encoding of activity durations.
- We present a comprehensive framework for evaluating the quality of model outputs. We use human interpretable distance metrics such that users can reasonably assess the suitability of models for various tasks.

# Synthesising Activity Participations and Scheduling with Deep Generative Machine Learning

Fred Shone<sup>a</sup>, Dr Tim Hillel<sup>a</sup>

<sup>a</sup>*University College London (UCL), Behaviour and Infrastructure Group (BIG), Chadwick Building, Gower Street, London, WC1E 6BT, United Kingdom*

---

## Abstract

Using a deep generative machine learning approach, we synthesise human activity participations and scheduling (the choices of what activities to participate in and when). Activity schedules, which represent what people do and when, are a core component of many applied transport, energy, and epidemiology models. Our data-driven approach learns the distributions resulting from human preferences and scheduling logic without the need for complex interacting combinations of sub-models and custom rules. This makes our approach significantly faster and simpler to operate than existing approaches to synthesise or anonymise schedule data. We additionally contribute a novel schedule representation and a comprehensive evaluation framework. We evaluate a range of schedule encoding and deep model architecture combinations. The evaluation shows our approach can rapidly generate large, diverse, novel, and realistic synthetic samples of activity schedules.

*Keywords:* Synthesis, Deep Machine Learning, Generative Machine Learning, Human Behavioural Modelling, Choice Modelling

---

## 1. Introduction

We propose a novel approach to an existing modelling challenge - the generation or *synthesis* of realistic samples of activity schedules. We define activity schedules as 24-hour-long sequences of activity type participations belonging to an individual, with associated start times and durations for each activity. Activity schedules are critical for many domains concerned with predicting or simulating human behaviour, such as Activity-Based Models and Agent-based simulations, including MATSim (Horni et al., 2016). In both cases, large samples of activity schedules are used to represent patterns of activities for representative populations of agents. Such models are used as decision-support tools for transport, energy and epidemiological scenarios.

Our definition of activity schedules can be decomposed into: (i) participations - *if or how many times an individual chooses to undertake certain activities*, and (ii) timings - *when and for how long to undertake the chosen activities*. Note, we do not consider other aspects such as activity locations or associated trips and their attributes, such as mode choices.

The participation and timing of multiple activities for an individual create a high-dimensional object with complex joint distributions. The complex distributions of ac-

tivity schedules are the result of the real-world processes by which people plan and undertake their days. This process includes the consideration of (i) physical and temporal constraints, such as not being able to partake in multiple activities at the same time or fitting all activities into a finite time budget, (ii) personal and social constraints, such as arriving at work on time or needing to buy food, (iii) individual preferences, such as the desire to participate in leisure activities or preferences towards different activity start-times, and (iv) interactions with others, such as coordinating shared activities in a household or via congestion.

The prevailing approach in both research and practice is to decompose the scheduling process into a series of discrete choices, applied sequentially. Each of these choices is conditioned on observed information, such as socio-economic attributes, and on previously made choices. To ensure temporal consistency, choices are then combined with rule-based scheduling algorithms. We highlight three main critiques of this approach: (i) sequential choices presume some order of decision making or causation that may be unrealistic, (ii) the combination of discrete choices and rules is simplified such that it cannot reproduce the real diversity of observed activity schedules, and (iii) the complex combination of multiple interacting sub-models and rules is challenging to develop, calibrate and use.

We demonstrate a novel approach for activity schedule synthesis using deep generative machine learning (ML). Our approach allows for the simultaneous synthesis of schedules, combining choices that would typically be made separately. Additionally, deep generative ML explicitly models the variation in observed data, without the need for conditional information. This results in three key benefits: (i) simultaneous synthesis potentially allows more realistic interaction of choice components, (ii) deep generative ML maintains diversity in output sequences, and (iii) in combination, the approach is simple and fast to apply. We comprehensively evaluate the quality of output activity schedules both individually and in aggregate.

A major current limitation of our approach is that we do not consider conditionality, such as in a typical behavioural modelling framework, for example, we cannot model responses to changes in socio-economic attributes or accessibility. This limits the application to where conditionality is not required, such as: (i) synthesis, (ii) data anonymisation, and (iii) diverse up-sampling.

Ultimately, this work is intended to demonstrate and progress generative modelling approaches in this domain, to enable their introduction into models and frameworks with conditionality in future. We share experimentation with data encodings and model architectures to assist future approaches using deep ML and generative approaches. Code for this research is available from Caveat<sup>1</sup>.

### 1.1. Activity Scheduling

Table 1 provides an overview of existing applied modelling frameworks that incorporate human activity scheduling. These approaches all make use of combinations of bespoke rules and statistical choice models to model schedules. These approaches seek to realistically model the activity scheduling process through the incorporation of realistic demand representation and generation processes. The incorporation of more realism has led to complex systems of interacting model components. Generally, these models

---

<sup>1</sup><https://github.com/big-ucl/caveat>

Table 1: Summary of Existing Activity Scheduling Approaches

Model/Framework	Activity Participation	Activity Timing
TASHA (Miller and Roorda, 2003)	Rule-based	Rule-based
ALBATROSS (Arentze and Timmermans, 2004)	Rule-based	Rule-based
FAMOS (Pendyala et al., 2005)	Nested-logit models	Hazard models
CEMPDAP (Sener et al., 2006)	Nested-logit models	Hazard models
ADAPTS (Auld and Mohammadian, 2009)	Rule-based	Rule-based
DaySim (Bradley et al., 2010)	Multinomial-logit models	Multinomial-logit models
SDS (Khan and Habib, 2023)	Markov Chain Monte Carlo	Rule-based

are slow and expensive to develop. For example, they typically require the collection of data describing all possible realisations of choice sets and significant human effort to calibrate.

A more theoretical critique of the above approaches is that they decompose schedule modelling into sequential choices. This presumes some order of decision-making that may be unrealistic. It is not clear, for example, if a person chooses to go shopping after work because they finished early, or if they finished early to go shopping. A common response to this is to combine discrete choices within joint models, such that they are modelled simultaneously.

[Pougala et al. \(2023\)](#) combine activity participation and scheduling into a simultaneous model. They achieve this via a simulated and sampled choice set. This approach is consistent with existing behavioural theory and is flexible enough to be extended to a variety of problems, constraints, and utility specifications. However, both estimation of the parameters and simulation of schedules are computationally expensive, limiting scalability. [Manser et al. \(2021\)](#) manage to scale the approach to application as part of an activity-based transport demand model, but they limit the scope of the simultaneous approach to activity timings only.

A core critique of existing approaches is that they under-represent the diversity of real behaviours. For example, tour-based approaches, such as used by [Miller et al. \(2005\)](#), restrict schedule activity participations to a reduced set of common patterns. By omitting less common behavioural patterns, these models introduce biases that limit their realism. Machine Learning (ML) approaches, such as used by [Koushik et al. \(2023\)](#) demonstrate the simultaneous modelling of participations and scheduling. However, by taking a discriminative approach, the model effectively generates the most likely activity sequence for each demographic group, therefore ignoring realistic variation within the groups. Such simplifications limit the realism of downstream models or simulations.

Activity schedules have also been treated purely as sequences with probabilistic transitions. For example, [Liu et al. \(2015\)](#) model activity sequences as Hidden Markov Models. Their approach allows consideration of both frequent and infrequent activities and resulting sequences. However, their work does not consider activity durations and is limited to the analysis and clustering of data rather than the generation of new sequences of activities.

### 1.2. Machine Learning Approaches to Activity Scheduling

Traditional approaches to discrete choice modelling are structured such that their parameters can be both constrained and interpreted to be consistent with behavioural the-

ories. However, increasingly researchers are applying purely data-driven ML approaches to these problems, including for schedule prediction.

[Nayak and Pandit \(2023\)](#) consider activity sequences (participations) across multiple days as a classification problem; comparing the performance of various bagging and boosting models for this task. They simplify the activity scheduling problem by identifying a reduced set of common day tours and then treating scheduling as a discriminative supervised learning problem. [Hafezi et al. \(2021\)](#) use Random Forests to predict activity start times and durations given person attributes. They then use heuristic rules to assemble these activity times and durations into schedules. Time is discretised into various bin sizes from 10 to 360 minutes. In such discriminative ML approaches, evaluation is made by reporting classification accuracy for various predefined clusters against ground-truth data. The use of accuracy for evaluation makes the impact of the approaches on a broader scheduling framework difficult to assess.

The above ML approaches tackle different components of a typical activity modelling framework - activity participations and timing. However, common to many traditional approaches, choices are discretised into simplified discrete sets, limiting realism, and requiring schedules to be assembled via multiple interaction models or heuristics.

[Koushik et al. \(2023\)](#) use a deep ML model to generate activity schedules for given agent attributes using recurrent neural networks (RNNs). Their model considers activity participations and their scheduling jointly as a simultaneous choice. They discretise 24-hour schedules into five-minute steps and consider nine different types of activity. They sample activities at each step based on maximum likelihood estimation, but do not include sampling in the inference process. As such, we do not consider this to be a generative model. Evaluation is made through the consideration of key selected marginal distributions, including the distribution of start times by type of activity. The authors find replicating aggregate realism challenging, particularly correctly representing short and infrequently observed activities. There is limited consideration of individual sample quality, or more broadly, of the distribution of their results.

In all cases, these models take a discriminative or conditional approach, where variation in observed schedules must be described by either explanatory variables or variation in arbitrary error terms (typically normal). Our work provides an alternative to the above by approximating the joint distribution of schedule activity participations and timings, and by explicitly synthesising variation by drawing from this joint distribution using a generative approach. This removes the need for explanatory data to explain observed variation.

### 1.3. Activity Schedule Evaluation

Generated activity schedule evaluation is typically performed through the comparison of aggregate distributions with a target sample of schedules. The models presented in Table 1 are primarily concerned with the representation of travel demand and therefore focus on the extraction and comparison of distributions such as total trip rates.

More recently, [Pougal et al. \(2023\)](#) and [Drchal et al. \(2016\)](#) make a more holistic evaluation through consideration of multiple marginal and conditioned distributions, such as different activity participation rates and start times.

A common evaluation approach involves analysing aggregate activity participation rates by time bin. Figure 1 shows this distribution for 2022 UK National Travel Survey

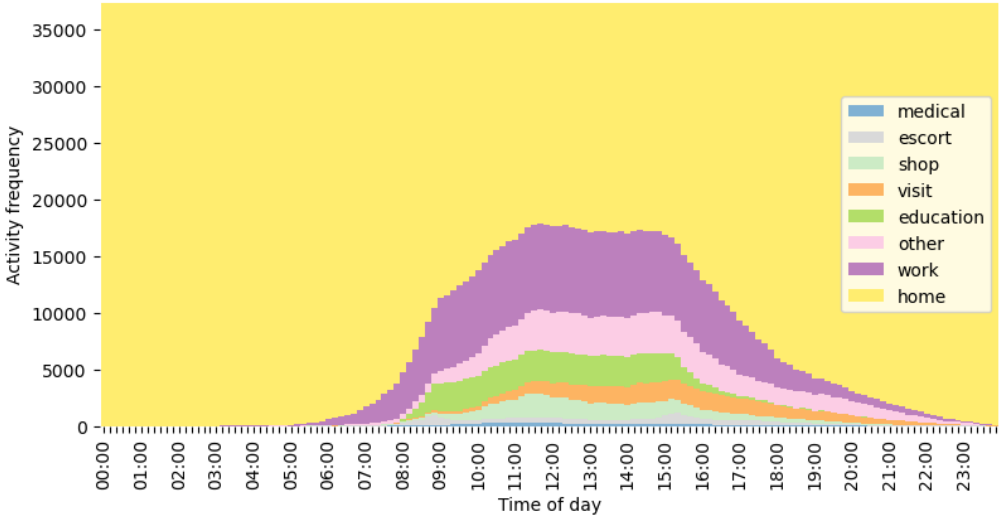


Figure 1: UK National Travel Survey (2021) Agg. Activity Participation by Time Bin

data. Such evaluation considers total or relative participation in activities by time of day. However, by aggregating individuals' choices, such evaluation can hide potentially unrealistic disaggregate behaviours. More generally, activity schedules are high-dimensional objects. Therefore more detailed analysis is needed to validate the realism of individual behaviours.

In the above works, individual schedule quality is either omitted or evaluated through visual inspection. Our work builds on the above by implementing a more comprehensive framework of distributions for evaluation, as well as proposing additional metrics considering individual schedule quality.

#### 1.4. Deep Generative Modelling

We define a generative model as a model that learns an approximation of a real data distribution, based on some observed sample of data from that distribution. A generative model can then be used to generate new, previously unobserved, samples by sampling from the modelled distribution.

Deep Generative Models (DGMs) make use of large training datasets and deep machine learning architectures to learn the distributions and joint distributions of complex high-dimensional data such as images, video, text and speech. Their depth allows for the learning of complex relationships, potentially learning excellent approximations of the real generation process. In this work, we demonstrate the application of DGMs for generating large samples of human activity schedules. There are many types of DGMs with various trade-offs briefly described below.

Auto-regressive models, such as PixelCNN by [Oord et al. \(2016\)](#), assume some ordering to predictions such that there is conditionality to previous estimates. Recurrent Neural Networks (RNNs), used to make sequential classifications, can be used as auto-regressive generative models, where at each step the model makes estimates given previ-

ously sampled estimates. This approach is popular in language modelling but assumes an order in the data generation process that may be unrealistic for scheduling.

Variational Auto Encoders (VAEs), originally proposed by [Kingma and Welling \(2013\)](#) and [Rezende et al. \(2014\)](#), are a form of latent variable model. During training, the model learns a mapping from the training data to a normally distributed latent space via an encoder model as well as a mapping from this latent space to estimates of the real distribution via a decoder model. After training, new samples can then be generated by sampling from the latent space and passing through the decoder. The VAE architecture provides a flexible and expressive framework, with demonstrated results in many complex learning domains such as images and language.

The above approaches use or estimate likelihood as a training objective. Generative Adversarial Networks (GANs), originally proposed by [Goodfellow et al. \(2014\)](#), discard this requirement, instead using a sample-based objective using a generator and discriminator architecture. This approach is extremely expressive, allowing the generation of highly realistic data. However, GANs do not estimate density and, as such, the likelihood of generated samples is not modelled. Training GANs is also difficult, as the generator-discriminator architecture can be unstable and prone to mode collapse.

Diffusion models, such as de-noising diffusion ([Ho et al., 2020](#)), split the generation process into multiple steps of noise removal. Performance is generally comparable to or better than VAEs or GANs, but more computationally expensive due to having many de-noising steps. More generally, flow-based approaches, such as normalising flows ([Rezende and Mohamed, 2015](#)), seek to more efficiently generate data through sequences of transformations, but finding or learning these transformations is often difficult.

We focus on VAEs in this work due to the requirement for good density estimation, i.e. the need to produce samples of schedules that are representative in aggregate, rather than individual sample quality. This benefit of VAEs is discussed by [Lucas et al. \(2019\)](#) and demonstrated by [Sajjadi et al. \(2018\)](#). Although VAEs are generally considered to have poorer individual sample quality than alternative approaches, we argue that this sample quality is likely adequate for schedule-generating tasks. VAEs are also preferable due to their relative speed, stability, and ease of training. In particular, they are less prone to mode collapse than GANs.

### 1.5. Evaluating Deep Generative Models

A common requirement of DGMs is probability density estimation, where good density estimation results in the modelled distribution being close to the distribution of the real data. Likelihood is typically used as a metric of closeness in statistical models. However, many deep learning models, including VAEs and GANs, do not have a tractable likelihood. As such, it is typically estimated from data samples.

As per [Theis et al. \(2016\)](#), estimating complex multi-dimensional probability distributions from samples is problematic. Assumptions about how probability density is estimated can bias results. More practically, reporting a single statistic for a high-dimensional generation problem limits feedback about how the model can be expected to perform or underperform in specific use cases.

DGMs are often found to exhibit a trade-off between individual sample quality and overall density estimation, described as precision and recall by [Sajjadi et al. \(2018\)](#) and as fidelity and diversity by [Naeem et al. \(2020\)](#). In some use cases, such as image generation,

sample quality is critical, and evaluation of density estimation is limited to ensuring there is sufficient diversity in generated outputs.

More broadly, as models only approximate real distributions, it is sensible to consider how their approximations impact performance for their intended application. For this reason, we propose several interpretable distance metrics for density estimation. These can be used to make qualitative evaluations of model suitability for various applications or combined to make quantitative comparisons between models.

### 1.6. Generative ML in Transport Modelling

Deep generative models have been applied for population synthesis tasks - the generation of joint attributes for a representative population of individuals. [Borysov et al. \(2019\)](#) apply a VAE architecture to population synthesis. They comprehensively evaluate the density estimation of models, comparing marginal, bi-variate and tri-variate distributions. They find their approach can outperform conventional methodologies in high-dimensional cases. [Kim and Bansal \(2023\)](#) add to this work, also using a GAN-based approach. They formalise a feasibility-diversity trade-off, where high feasibility is the avoidance of infeasible samples, and high diversity improves the generation of missing data. They show that the model can recover missing samples.

Deep generative models have also been used to generate activity schedules. [Liao et al. \(2024\)](#) discretise schedules into 15-minute steps. They use a complex deep autoregressive model to generate schedules and associated activity locations conditional on a range of socio-economic attributes for members of households. They evaluate generated schedules by comparing a small set of marginal distributions and demonstrate the generated schedules in a downstream traffic simulation task. An attention-based architecture outperforms various RNN architectures, although an LSTM architecture compares similarly.

[Badu-Marfo et al. \(2020\)](#) use a GAN to generate both synthetic attributes and sequences. They additionally train their model to allow differentiable privacy. They show promising results for marginal attribute distributions, but find that the model performs poorly at scheduling. They note that the model struggles with the complexity of learning higher-order correlations and long-range temporal dependencies.

[Kim et al. \(2022\)](#) use a conditional GAN architecture to predict trip purpose and socio-demographic attributes from smart card data. The use of a generative model explicitly allows for variance in the model predictions. They compare transformer architectures with temporal and spatial encodings against baseline approaches. Evaluating the model using marginal and bivariate distributions, they find that the GANs do not outperform benchmark methods. However, through further evaluation of fidelity, diversity, creativity, and accuracy, they identify some performance benefits of GANs.

We add to the above by applying VAEs to simultaneous activity participations and scheduling. We consider novel combinations of schedule encodings and model architectures. We also introduce a comprehensive evaluation framework, designed to evaluate the suitability of generated schedules for downstream tasks.

### 1.7. Generative ML for Sequence Data

Activity schedules can be considered as sequence data, similar to text. Language models represent text as sequences of tokens representing words or parts of words, and generate new text in an auto-regressive manner. A key challenge of language models is

the consideration of long-range dependencies, leading to the development of architectures suited to the retrieval of information over very long sequences of text, such as by [Vaswani et al. \(2017\)](#).

[Bowman et al. \(2015\)](#) demonstrate a sequence-generating VAE that can generate text by sampling from the latent space. They note this is effectively a combination of an auto-regressive and latent model. They show that the latent representation can learn useful information about the overall distribution of text. Variations of this architecture are used by [Gregor et al. \(2015\)](#) for generating images, and [Roberts et al. \(2018\)](#) for generating music. In some cases, models are evaluated on the Kullback–Leibler Divergence (KLD) of their latent layer and regeneration of test sequences; however, this is primarily used for model comparison. Ultimately, researchers employ qualitative evaluation of models based on intended application.

Activity schedules are sequences of joint activities and durations, which create a novel mixed data type. Schedules combine both categorical information for activities, as per text data, and continuous information for durations, as per image pixel values. Schedules also typically have a fixed total duration.

### 1.8. Research Contributions

In this paper, we contribute a novel approach to synthesising activity schedules using deep generative models. More specifically:

- We contribute a novel approach to synthesising human activity schedules using deep generative modelling that allows for the rapid synthesis of large, realistic samples of human activity schedules.
- We propose a novel activity schedule encoding, using a continuous encoding of activity durations.
- We present a comprehensive framework for evaluating the quality of model outputs using human-interpretable distance metrics such that users can reasonably assess the suitability of models for various tasks.

We additionally provide a comparison of different schedule encodings and VAE encoder/decoder architectures to assist further research into the modelling of activity schedules. Our work is reproducible using [Caveat](#)<sup>2</sup>.

## 2. Methodology

### 2.1. Informal Problem Definition

We consider a sample of schedules, drawn from a population, such that it is representative. This sample would typically represent schedules from a population of individuals for a single day, such as from a structured travel demand survey. However, it could also represent any population or subset, such as multiple schedules from the same respondents or schedules for a particular demographic. For generality, we therefore do not specify the population or application within this paper.

---

<sup>2</sup><https://github.com/big-ucl/caveat>

Our goal is to use this sample to approximate the distribution such that we can draw new synthetic samples of schedules that are representative of the original population, where representativeness concerns both the realism of individual schedules and the collective distribution of all schedules in the sample.

### 2.2. Activity Schedule Definition

We define a single activity schedule  $x$  as an ordered sequence of activity types  $a_n$  with associated durations  $d_n$ :

$$x = [(a_1, d_1), (a_2, d_2), \dots, (a_N, d_N)], \quad (1)$$

where  $n$  indexes the position in the schedule. The number of activities in the schedule (i.e. the sequence length  $N$ ) may vary, but the total duration should equal the time period  $T$ , such that:

$$\sum_n^N d_n = T. \quad (2)$$

We use a time period  $T$  of 24 hours, starting and ending at midnight. However, the approach can be trivially extended to different periods and durations.

### 2.3. Problem Definition

We consider a sample of schedules to be a random variable  $X \subset \mathcal{X}$ , where  $\mathcal{X}$  is the space of all possible activity schedules. These schedules are drawn from a target distribution  $P_X$ , such that we consider them to have the same distribution, which we refer to as the *real distribution*. This distribution captures the process of human activity scheduling, encompassing both individual preferences and environmental constraints such as accessibility and congestion.

Let the *real sample* be a finite set of  $N_{real}$  observed schedules:

$$\mathcal{S}_{\text{real}} = \{x_1, x_2, \dots, x_{N_{\text{real}}}\} \subset \mathcal{X}, \quad \text{with } x \sim P_X. \quad (3)$$

$\mathcal{S}_{\text{real}}$  is used to train a generative model  $P_\theta$ , parametrised by  $\theta$ , which aims to approximate the real distribution  $P_X$  with a learned distribution  $\hat{P}_X$ .

From the trained model, we generate a *synthetic sample* of  $N_{syn}$  schedules:

$$\mathcal{S}_{\text{syn}} = \{\hat{x}_1, \hat{x}_2, \dots, \hat{x}_{N_{\text{syn}}}\}, \quad \text{with } \hat{x} \sim \hat{P}_X. \quad (4)$$

The modelling objective is for the learned distribution  $\hat{P}_X$  to closely approximate the real distribution  $P_X$ , such that:

$$\hat{P}_X \approx P_X. \quad (5)$$

Note that the distribution  $\hat{P}_X$  includes the density, or probability, of all possible activity schedules and the joint distributions within each schedule. As per the real sample, these are for *realised* schedules, accounting for preferences and constraints. For all the following experiments, we choose the size of the synthetic sample ( $N_{real}$ ) to match the size of the real sample ( $N_{syn}$ ).

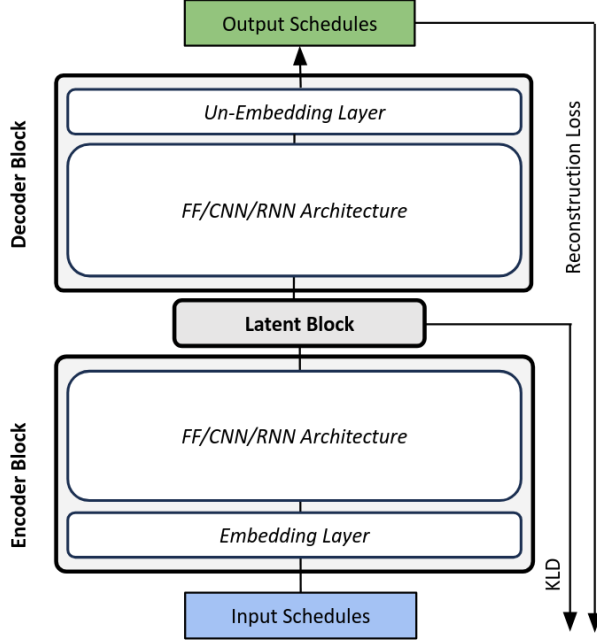


Figure 2: VAE Models Template

#### 2.4. Generative Modelling with Variational Auto-encoders

We use the Variational Auto-encoder (VAE) as our deep generative modelling approach. Each VAE model is composed of an encoder block, a latent block, and a decoder block as per Figure 2. The various VAE encoder/decoder block architectures are detailed in Section 4.

We use VAEs to generate each schedule  $x \in \mathcal{X}$  conditionally on a latent variable  $z$ . The generative process is modelled as a conditional distribution  $P_\theta(X | Z)$ , where the latent space  $Z$  is a (multivariate) standard normal,  $P(Z) = \mathcal{N}(0, I)$ .

During training, an *encoder block* learns a mapping from input schedules to the latent distribution. This is commonly referred to as the *inference model*  $Q_\phi(Z | X)$ . This model is responsible for mapping the real distribution of schedules to the latent space and, therefore, for learning the distribution of inter-schedule variation.

The *decoder block* simultaneously learns a mapping from the latent space to output schedules. This is commonly referred to as the *generative model*  $P_\theta(X | Z)$ . This model is effectively responsible for learning the distribution of intra-schedule variation, such as temporal dependencies.

To learn both the inference and generative processes, VAEs use two loss functions with two aims: (i) to reconstruct schedules passed through the entire encoder-latent-decoder structure, and (ii) to distribute the latent layer as a standard normal distribution.

For the former, reconstruction loss (ReconLoss), measures the difference between each output schedule and the target input schedule. Reconstruction losses are described in Section 4.3. For the latter, Kullback-Leibler Divergence (KLD) loss measures the difference between the latent layer distribution and the target normal distribution. The

final loss function is composed of ReconLoss and KLD, where KLD is factored using the hyperparameter  $\beta$  (reported separately for each model in Table 4).

$$\text{Loss} = \text{ReconLoss} + \beta \text{KLD}$$

After training, synthetic schedules are generated by first sampling  $z$ , then decoding  $\hat{x} \sim P_\theta(X | z)$ . This two-step process allows the model to capture both: (i) *Inter-schedule diversity*, through variation in the latent space  $Z$ , and (ii) *Intra-schedule structure*, through the conditional generation process  $P_\theta(X | Z)$ . The sampling of  $Z$  is independent, such that there are no dependencies between schedules.

The intuition behind the VAE is that, by learning a good mapping from a known continuous latent space to the real sample of schedules. New schedule samples, with a similar distribution to the real sample, can be drawn by sampling from the latent space. For more details and a derivation of the VAE model structure and loss function, please refer to [Kingma and Welling \(2019\)](#).

### 2.5. Observed Data

For the real sample of schedules, we extract and filter 59,265 24-hour trip diaries from the 2023 UK National Travel Survey (NTS) trips table<sup>3</sup>. We convert this trip data into schedules using PAM ([Shone et al., 2024](#)). We simplify the real schedules by: (i) removing trips, and (ii) simplifying activity types to the set {home, work, education, medical, escort, other, visit, shop}. To remove trips, we extend the prior activity durations to include the following trip duration, such that activity start times are maintained. In effect, the following work therefore models combined activity and following trip durations. However, for conciseness, we describe this more simply as activity durations throughout. The practical implication of this is that if subsequently modelling trips, the activity duration can be treated as a budget for both the travel time and the activity participation duration.

To artificially create structural zeros within the observed data, which we later use for quantitative sample quality evaluation, the schedules are: (i) filtered to exclude non-home-based schedules (schedules that do not start and end at home), and (ii) modified, such that consecutive home, work or education activities are combined into single activities of the same type with combined duration. Figure 3 shows example activity sequences from the UK NTS.

### 2.6. Experiment Design

We train and evaluate six different VAEs with different combinations of: (i) schedule encoding, and (ii) model architectures. These models and their naming are summarised in Table 2.

We consider two schedule encodings: (i) Discrete, and (ii) Continuous. These encodings are detailed in Section 3. We consider three model architectures: (i) Feed-Forward (FF), composed of fully connected layers, (ii) Convolutional (CNN), and (iii) Recurrent (RNN). These architectures are detailed in Section 4.

Our evaluation framework is described in Section 5. This evaluation is used for high-level comparison of schedule encodings and model architectures in Section 6, and more

---

<sup>3</sup><https://ukdataservice.ac.uk>

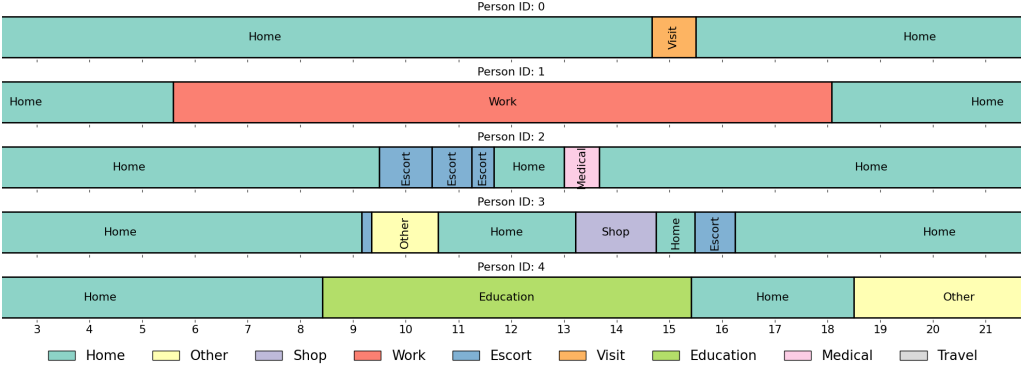


Figure 3: Example NTS Schedules

Table 2: Experiments Overview

Model Name	Short Name	Schedule Encoding	Architecture
Discrete FF	DiscFF	Discrete	Feed-Forward (FF)
Discrete CNN	DiscCNN	Discrete	Convolutional (CNN)
Discrete RNN	DiscRNN	Discrete	Recurrent (RNN)
Continuous FF	ContFF	Continuous	Feed-Forward (FF)
Continuous CNN	ContCNN	Continuous	Convolutional (CNN)
Continuous RNN	ContRNN	Continuous	Recurrent (RNN)

detailed consideration of the best-performing models in Section 7. We supplement these results with different scenarios, considering data sample sizes in Section 8 and alternative COVID-19 behaviours in Section 9.

Our experiments are intended to demonstrate: (i) the application of a generative modelling approach to human activity scheduling, and (ii) the impact of schedule encoding and model architecture on schedule generation quality.

### 3. Schedule Encodings

We consider two different schedule representations: (i) a classic discrete encoding, and (ii) a novel continuous encoding.

#### 3.1. Discrete Schedule Encoding

Individual activity schedules are typically encoded as discretised sequences, such as per Koushik et al. (2023). Each schedule is composed of a fixed-length vector of categorical tokens, where each token represents participating in a specific activity type for some fixed time step of duration  $t$ . We use a 10-minute time step. Where a time step contains multiple activities, for example, when a schedule transitions from one activity to another, or for a very short activity, we choose the activity with the greatest duration within that time step. Figure 4 shows an illustrative example of this encoding.

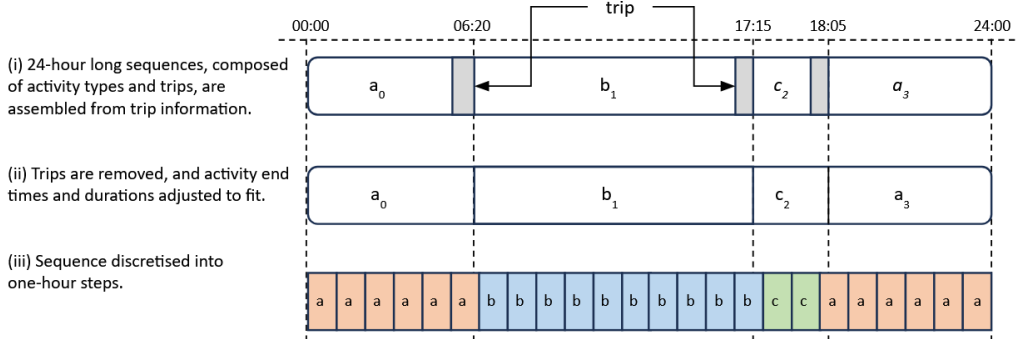


Figure 4: Discrete Activity Schedule Encoding

### 3.2. Continuous Schedule Encoding

The discrete schedule encoding is simple to implement but limits temporal precision to that of the time step duration  $t$ . This impacts short-duration activities disproportionately, potentially removing them entirely from an encoded schedule. Reducing the step duration improves this precision but increases the encoding length. Conversely, long-duration activities are represented by many consecutive tokens representing the same activity. This is inefficient and makes correct duration prediction harder because a single wrong step cuts an activity in two, dramatically changing the schedule. We therefore propose a more precise and compact schedule encoding, representing schedules as sequences of activity types with corresponding continuous durations.

All schedule sequences start with a special *start of sequence* token, followed by encodings of each activity with the associated duration. We fill the remainder of the sequence with special end-of-sequence tokens up to a maximum total sequence length. We set the maximum total sequence length to be 16, allowing for schedules with up to 15 different activities.

This approach is based on language encoding; however, it differs in that it uses a two-dimensional token. The first dimension of each token is a categorical encoding of activity type, and the second is a continuous value between 0 and 1 that represents the activity duration in days. The start and end of sequence tokens are given a duration of zero. Figure 5 shows an illustrative example of this encoding. We refer to this as the continuous representation because it uses a continuous representation of time.

## 4. Model Design

All models are based on a template as per Figure 2, composed of a latent block (Section 4.1), an encoder block and a decoder block. Depending on the schedule encoding, VAE encoder/decoder blocks use either discrete or continuous embedding and un-embedding layers as per Section 4.2, and alternative reconstruction losses as per 4.3. The various encoder/decoder block architectures are described in Section 4.4. Specific language used in the following sections is defined in the mini glossary in Table 3.

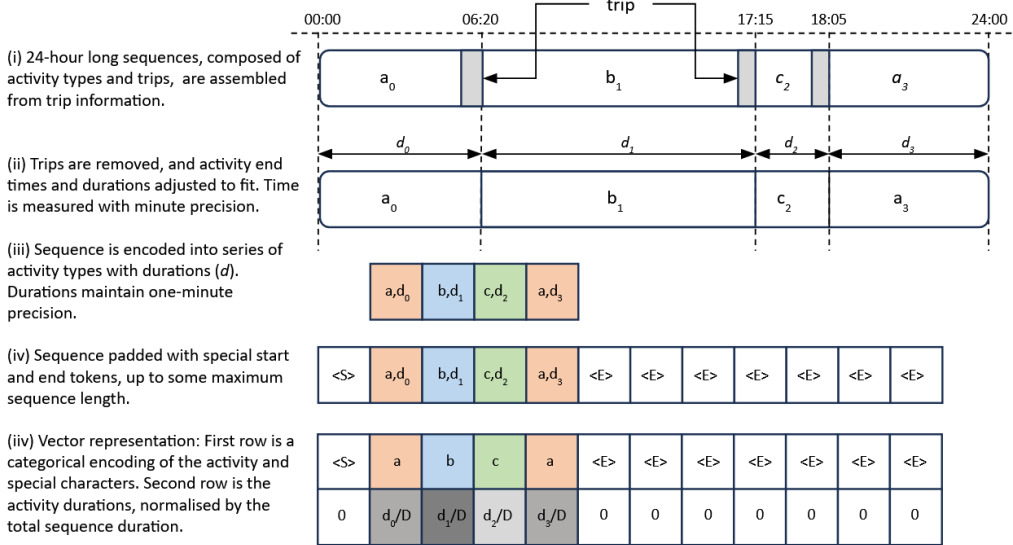


Figure 5: Sequence Activity Schedule Encoding

Table 3: Model Design Glossary

Definition	
Adam	Optimisation algorithm used for gradient descent
CNN	Convolutional Neural Network
Drop-out	Layer to randomly set proportion of gradients to zero during training
Embedding	Layer to transform input embeddings into vector representation
Feed-Forward (FF)	Fully connected layers
Flatten	Operation to reduce dimensionality of input tensor
KLD	Kullback-Leibler Divergence
LeakyRELU	Activation function to add non-linearity
LSTM	Long Short-Term Memory, a type of RNN
Reconstruction Loss	Distance between input schedule and output schedule
Resize	Layer to resize input tensor using a fully connected linear layer
RNN	Recurrent Neural Network
Tensor	Multi-dimensional array
Un-embedding	Layer to transform input into an array of activity and duration predictions
Unflatten	Operation to increase dimensionality of input tensor
VAE	Variational Auto Encoder

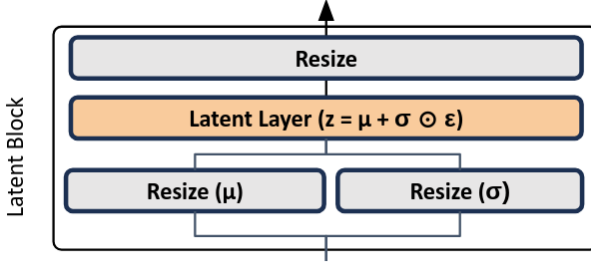


Figure 6: Latent Block

#### 4.1. Latent Block

Figure 6 presents the latent block structure in all models. Within the block, the latent layer, a vector of length six, is sampled from a normal distribution with mean  $\mu$  and standard deviation  $\sigma$ . This is commonly referred to as the *reparametrisation trick*.  $\mu$  and  $\sigma$  are both vectors with the same size as the latent layer.  $\mu$  and  $\sigma$  are resized from the encoder output using fully connected linear layers. After sampling, the latent layer is resized as required using a fully connected linear layer for passing into the decoder block.

#### 4.2. Embedding and Un-Embedding

The discrete and continuous schedule encodings require different embedding designs. In both cases, embedding is used to transform the input sequence encodings into two-dimensional representations. The first dimension represents the sequence length, and the second is the embedding size. In all cases, we choose the embedding size to match the layer size of the encoder/decoder architecture, reported for each model in Table 4.

##### 4.2.1. Discrete Embedding and Un-Embedding

Models using the discrete schedule encoding use a standard learnt embedding layer to embed each input activity token as a vector. These are then stacked to create a two-dimensional representation for each schedule.

Un-embedding reverses the operation using soft-max and then sampling the highest value at each time step. Note that in all cases, we find sampling the highest probabilities at each step outperforms weighted sampling.

##### 4.2.2. Continuous Embedding and Un-Embedding

Models using the continuous schedule encoding use a custom embedding that embeds the first dimension (activity type token) of the input data into vectors using a learn embedding layer as above. The resulting activity embedding vectors are then concatenated back to their durations. This combines both a categorical and continuous embedding.

The continuous encoding is un-embedded by the decoder following a similar process in reverse. A vector of durations for the sequence is separated and passed through a sigmoid activation so that all duration values are between zero and one. The remaining vectors are decoded into activities using a soft-max layer and sampling the highest value at each step. Activities and their durations for each sequence are then concatenated back together. After discarding padding tokens, durations for each sequence are normalised such that they sum to one.

### 4.3. Reconstruction Losses

The discrete embedding uses the mean cross-entropy of all predictions as reconstruction loss. The final loss function for the discrete encoding-based models is therefore:

$$\text{Loss} = \text{CrossEntropy}_{\text{activities}} + \beta \text{KLD}$$

The continuous encoding uses a combination of mean cross-entropy loss for the activity prediction and mean squared error for the duration prediction. We introduce an additional hyperparameter  $\alpha$ , detailed in Table 4, to weight the duration component of loss.

$$\text{Loss} = \text{CrossEntropy}_{\text{activities}} + \alpha \text{MSE}_{\text{durations}} + \beta \text{KLD}$$

### 4.4. Encoder/Decoder Block Architectures

The following section overviews the Feed-Forward, Convolutional and Recurrent VAE architectures. The number of blocks ( $N$ ) and their size ( $S$ ) vary for each model and are summarised in Table 4. The full architectures are available from Caveat<sup>4</sup>.

#### 4.4.1. Feed-Forward (FF) VAEs

The Feed-Forward (FF) architecture is presented in Figure 7. Both encoder and decoder blocks reshape inputs or outputs as required to make use of  $N$  feed-forward blocks. Each feed-forward block is composed of: (i) a fully connected linear layer of size  $S$ , (ii) a batch normalisation layer, (iii) a LeakyRELU activation layer, and (iv) dropout.

#### 4.4.2. Convolutional (CNN) VAEs

The Convolutional (CNN) model architecture is presented in Figure 8. The encoder layer uses  $N$  convolutional blocks, each composed of: (i) a one-dimensional convolutions layer of size  $S$ , with stride two and convolution size four, (ii) a batch normalisation layer, (iii) a LeakyRELU activation layer, and (iv) dropout. The two-dimensional output is then flattened for the construction of the latent block.

The decoder uses  $N$  de-convolutional blocks, each as per the above convolutional blocks but using de-convolutions rather than convolutions, also of size  $S$  with stride two and convolution size four. By carefully choosing output padding, the deconvolutional blocks upsample the latent layer to the required decoder output size.

#### 4.4.3. Recurrent (RNN) VAEs

The Recurrent (RNN) model architecture is presented in Figure ???. The encoder layer uses  $N$  stacked Long-Short Term Memory (LSTM) units of size  $N$  (Hochreiter and Schmidhuber, 1997). The block iteratively progresses through the input embeddings, and each LSTM unit passes a learnt hidden state as input to the next. The final output hidden state is then flattened as required for the latent block.

The decoder uses a similar structure in reverse. The output from the latent block is reshaped into the hidden state of the first decoding LSTM unit. This first unit is given the start of sequence token as input, further steps then use the sampled output from the

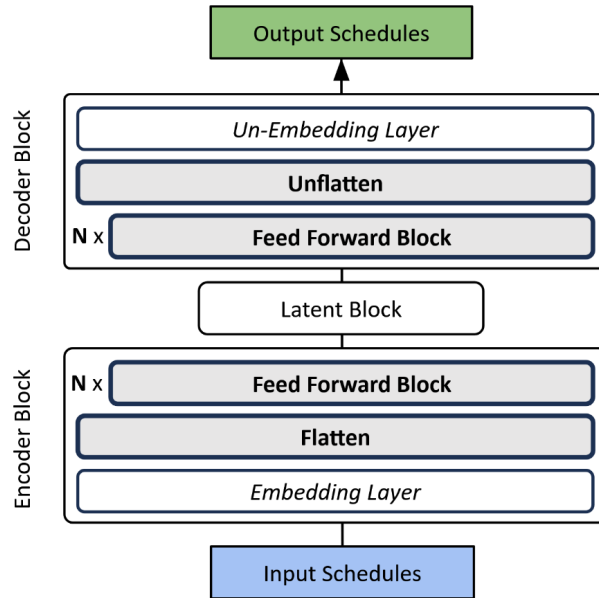


Figure 7: Feed-Forward Based VAE Template

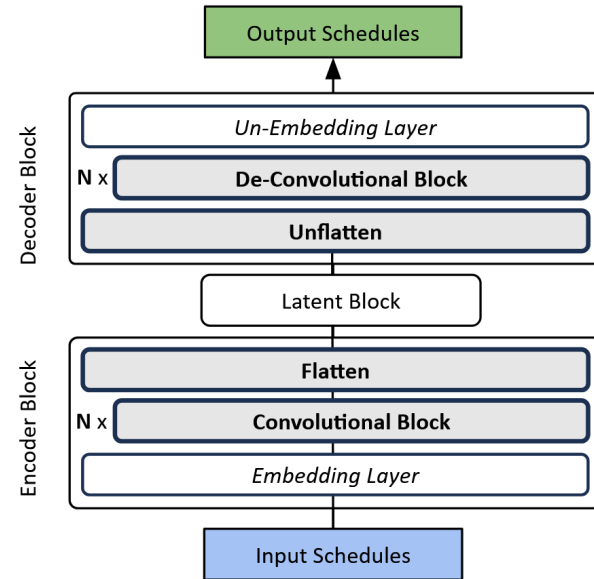


Figure 8: Convolutional Based VAE Template

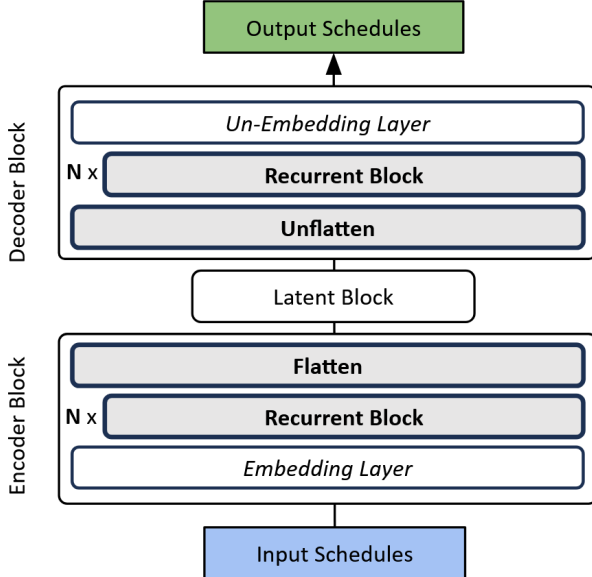


Figure 9: Recurrent Based VAE Template

previous step. During training, we use 50% teacher forcing, where previous predictions are replaced by training data, to improve training stability.

We sample activity predictions using argmax. This approach means that the decoder block is deterministic based on input from the latent layer, so variation from the generative process only relies on sampling the VAE latent layer. Incorporating probabilistic sampling into the decoder RNNs (i.e. autoregressive generation) does not improve performance.

#### 4.5. Model Training and Hyperparameters

Models are trained on 90% of the real sample data. We use the remaining 10% for validation during training. We train models until validation loss stabilises, typically for around 100 epochs. We do not find models suffer from over-fitting, likely due to the VAE design, which adds a stochastic process to training. We use Adam for gradient descent. Model training hyperparameters are reported in Table 4. The hyperparameters are chosen to optimise validation loss using the Tree-structured Parzen Estimator by Optuna (Akiba et al., 2019).

## 5. Evaluation Methodology

In this section, we consider the evaluation of the synthetic samples of activity schedules  $\hat{X}$ . Our aim is for the synthetic distribution  $\hat{P}_X$  to be equal to the real distribution  $P_X$ . This represents the ability of a model to correctly estimate the probability of

---

<sup>4</sup><https://github.com/big-ucl/caveat>

Table 4: Models Overview

Model	Block Size (NxS)	Latent Size	Learning Rate	Batch Size	$\beta$	$\alpha$	Drop Out
DicsFF	3x32	6	0.001	1024	0.005	-	0.1
DiscCNN	6x512	6	0.01	1024	0.005	-	0.1
DiscRNN	4x512	6	0.001	1024	0.01	-	0.1
ContFF	4x128	6	0.0001	1024	0.01	200	0.1
ContCNN	5x128	6	0.001	1024	0.01	200	0.1
ContRNN	4x256	6	0.001	1024	0.01	200	0.1

any possible activity schedule - commonly called *density estimation*. We estimate both  $P_X$  and  $\hat{P}_X$  by extracting marginal distributions and comparing these between the real and synthetic samples using a distance metric. We choose marginal distributions with qualitative meaning such that we can assess the implications of the quality of density estimation on specific tasks. We consider many marginal distributions such that when distances are aggregated, we can make a reasonable quantitative evaluation of overall density estimation. Density estimation is detailed in Section 5.1.

Perfect density estimation would satisfy our requirement for both individual schedule quality and aggregate representation across multiple schedules. However, because we can only estimate densities and because perfect estimation is not feasible, we supplement evaluation by additionally considering metrics for individual *sample quality* (Section 5.2) and *creativity* (Section 5.3).

### 5.1. Density Estimation Evaluation

Our evaluation of density estimation is composed of many marginal distributions as detailed in Table 5. Distributions are arranged in three domains:

- *Participations* which describe the participation in activity types.
- *Transitions* which describe the order of activity type participations.
- *Timings* which describe when activity types happen and their durations.

#### 5.1.1. Marginal Distributions

Within each domain, there are multiple types of marginal distributions, each typically further segmented by activity type or types as detailed in Table 5.

The participations domain considers the distributions of (i) sequence lengths - the number of activities in each schedule, (ii) *single* activity participation rates - the number of times an activity of each type occurs in each schedule, (iii) and *paired* activity participation rates - the number of times pairs of activities take place in each schedule.

Sequence lengths give a quick overview of if a model is generally over or under-generating activities. Single participation rates consider the occurrences of each type of activity. We use rates rather than probability so that the occurrence of activities more than once in a schedule is also considered. For example, a schedule with a *work* participation rate of two would have two distinct work activities. Paired activity rates

consider the occurrences of pairs of activities within the same schedule. Note that paired activity participations do not need to be consecutive, for example, the schedule *home - work - home* contains two pairs; *home + work* twice and *home + home* once. The consideration of non-consecutive pairs allows consideration of more complex dependencies within schedule activity participations, such as for escort and return escort trips.

The transitions domain considers schedule ordering as the distributions of sequences of activities. We consider sequences of two, three, and four consecutive activities, which we call bi, tri, and quad-grams. For example, the schedule *home - work - home* contains two bi-grams; *home to work* and *work to home*, and a single tri-gram *home to work to home*. Longer transition sequences allow consideration of longer-term dependencies within schedules.

Both participation and transition distributions are measured as *rates*, which are counts of occurrences for each schedule. We then consider the distribution of such rates across the whole sample. The left-hand side of Figure 10 shows an illustrative example of rate distributions for a real and synthetic sample of schedules.

Timing density estimation considers the distributions of different activity type start times and durations. Note that start times and durations are segmented by activity types enumerated by position in each schedule. This allows for the sensible consideration of timing within a sequence, for example, the first home activity, *home0* is distinguished from subsequent home activities, *home1*, *home2* and so on. We use days as a measure of time (and duration).

We additionally consider two bivariate distributions: (i) joint start time and duration, segmented by the activity type, which we call *start-durations*, and (ii) consecutive activity durations, segmented by the first activity type, which we call *consecutive-durations*.

Bivariate or *joint* distributions allow the consideration of more complex patterns. Start-durations consider the relationships between activity start times and durations, for example, if earlier start times are typically associated with longer durations for a particular activity type. Consecutive-durations consider the relationship between an activity duration and the duration of the following activity, for example, if a short duration is typically followed by another short duration for a particular activity type.

Figure 10 illustrates *rate* (left-hand-side) and *time* (right-hand-side) marginal distributions. Rates are ordinal, and timings are continuous. However, the time distributions are binned at five-minute intervals to reduce computational complexity. All distributions are described using mean density, which can be interpreted as the expected rate or time.

### 5.1.2. Distances

Because it is not possible to measure the likelihood of the synthetic sample and real sample have the same distribution, we instead measure the distances between their marginal distributions as a proxy. This has the benefit of allowing for interpretable metrics, but also allows for quantitative evaluation, as lower is always better.

Distances between the real and synthetic distributions are measured using Earth Movers Distance (EMD). EMD is symmetric with meaningful values, such that we can reasonably interpret them. For example, a distance of 0.1 for *work* activity *participation* rate can be interpreted as an expectation of 0.1 fewer or more of *work* activities occurring in each schedule. Similarly, a distance of 0.5 for an activity *start* can be interpreted as that activity starting, on average, half a day late or early. For bivariate distributions, we use L1 distance (also known as Manhattan/city-block distance).

Table 5: Summary of Distributions used for Density Estimation Evaluation

Domain	Marginal Distribution Description	Segmentation	Units	Descriptive Metric
Participations	Sequence Lengths	-	counts	av. length
	Single	home		
		work		
		education		
		shop	rates	av. rate
	Pair	:		
		home, home		
		home, work		
		home, shop		
		shop, shop	rates	av. rate
Transitions	Bi-gram	shop, shop		
		:		
		home-work		
		work-home		
		work-shop		
	Tri-gram	shop-shop	rates	av. rate
		:		
		home-work-home		
		home-work-shop		
		home-shop-work		
Timings	Quad-gram	shop-shop-shop	rates	av. rate
		:		
		home-work-shop-home		
		home-shop-work-home		
		home-shop-shop-home		
	Start times	home-shop-shop-shop	rates	av. rate
		:		
		home0		
		home1		
		work0	days	av. time
Consecutive-durations	Durations	:		
		home0		
		home1		
		work0		
		:		
	Start-durations	days	days	av. time
		home		
		work		
		education		
		:		

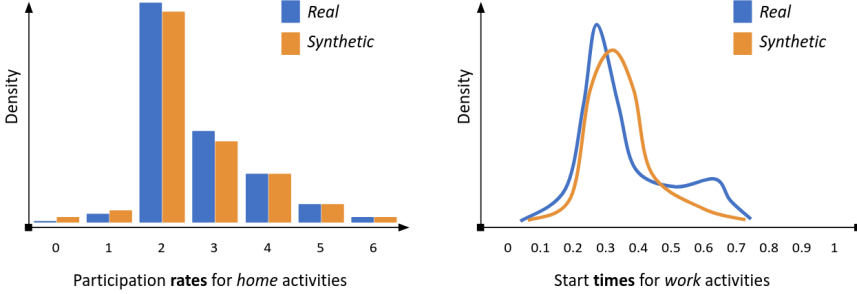


Figure 10: Illustrative Marginal Distributions

### 5.1.3. Approximating Density Estimation

Our approach of considering multiple types of marginal distributions with segmentation creates a large number of distances. Combined, these distances can give an approximation of overall density estimation. Segmented distribution distances are combined using frequency-weighted averages to provide summary metrics at the distribution level. These distribution distances can then be averaged to provide domain-level summaries. We do not further combine the three domain-level metrics as they have different units and meanings. Additionally, the domains allow qualitative consideration of model evaluations for different types of tasks, which may prioritise evaluation of one domain, such as times, over another.

### 5.2. Sample Quality Evaluation

It is possible to have good density estimation but poor individual schedule quality. To evaluate this quantitatively, we impose structure on our real sample (and therefore training data) by: (i) removing schedules that are not *home-based* (i.e. that do not start and end with home activities), and (ii) combining consecutive home, work and education activities. We can then report the probability that synthetic schedules are structurally correct, based on them being both *home-based* and not having consecutive home, work or education activities. We call this measure of sample quality *validity* and use the probability that a schedule is *invalid* as a distance metric, such that lower is better.

To account for schedules that have been previously observed by the model in the training data (and are therefore known to be structurally correct), we only report the sample quality of novel schedules - those not previously observed in the training data.

### 5.3. Creativity Evaluation

We are additionally interested in the model's ability to generate both (i) a good *diversity* of schedules – i.e. different from one another, as well as (ii) *novel* schedules – i.e. unique from schedules in the real sample. Diversity can be considered as a type of density evaluation metric, but is also used to specifically check if the model is suffering from mode collapse, a common issue with deep generative models, where they learn to generate an unrealistically reduced set of common outputs. We define diversity as the probability that a schedule is unique in the synthetic sample.

Table 6: Quality and Creativity Evaluation Definitions

Feature	Description
Invalidity	Probability that a schedule is not home-based or contains consecutive home, work or education activities.
Homogeneity	Probability of a sequence within the synthetic sample <b>not being</b> unique.
Conservatism	Probability of a sequence <b>occurring</b> in the training sample.

Table 7: Evaluation Summary

	Discrete			Continuous			Unit
	FF	CNN	RNN	FF	CNN	RNN	
<b>Density Estimation</b>							
Participations	0.152	0.162	0.817	0.062	<b>0.046</b>	0.064	rate EMD
Transitions	0.008	0.006	0.165	<b>0.004</b>	0.005	<b>0.004</b>	rate EMD
Timing	0.051	0.044	0.210	0.056	0.055	<b>0.025</b>	days EMD
<b>Sample Quality</b>							
Invalidity	<b>0.000</b>	<b>0.000</b>	0.050	0.057	0.030	0.018	prob.
<b>Creativity</b>							
Homogeneity	0.468	0.507	0.931	0.153	0.348	<b>0.022</b>	prob.
Conservatism	0.100	0.118	0.351	0.011	<b>0.010</b>	0.012	prob.

It is additionally desirable for our model to synthesise schedules unseen in the training data, which we define as novelty. We define novelty as the probability that a schedule is unique from the real sample. Note that the evaluation of schedule times and durations uses one-minute precision, such that synthetic samples from the discrete embedded models, which use a ten-minute precision, are structurally biased to be less creative.

To be consistent with density estimation, where lower is better, we define homogeneity and conservatism as the opposites of diversity and novelty (as described in Table 6), for use as evaluation metrics, such that lower is better.

## 6. Results

We first summarise and compare all models at a high level. The density estimation of two selected models, the Discrete CNN and Continuous RNN, is then evaluated in more detail in Section 7. Results are supplemented with various scenarios in Sections 8 and 9 using our preferred model, the Continuous RNN.

Table 7 presents a summary of domain density estimations, sample quality and creativity for the six models. We present distances such that lower metrics are better. Models have stochastic results both from the training process and from sampling the latent space. We therefore present all evaluation descriptive and distance metrics as means from five model runs. Variance is presented in a more detailed evaluation in Section 7.

Table 8: Density Estimation Evaluations

	Discrete			Continuous			Unit
	FF	CNN	RNN	FF	CNN	RNN	
<b>Participations</b>							
Lengths	0.363	0.399	2.100	0.140	<b>0.100</b>	0.154	rate EMD
Participation	0.079	0.078	0.301	0.040	<b>0.033</b>	<b>0.033</b>	rate EMD
Pair particip.	0.014	0.011	0.052	0.005	0.005	<b>0.004</b>	rate EMD
<b>Transitions</b>							
2-gram	0.020	0.015	0.145	0.009	0.010	<b>0.008</b>	rate EMD
3-gram	0.004	0.003	0.136	<b>0.002</b>	0.003	<b>0.002</b>	rate EMD
4-gram	0.002	0.002	0.213	<b>0.001</b>	0.002	<b>0.001</b>	rate EMD
<b>Timing</b>							
Start times	0.022	0.018	0.028	0.032	0.033	<b>0.016</b>	days EMD
Durations	0.039	0.034	0.215	0.041	0.039	<b>0.016</b>	days EMD
Start-durations	0.073	0.067	0.401	0.071	0.072	<b>0.031</b>	days EMD
Joint Durations	0.070	0.057	0.196	0.078	0.075	<b>0.038</b>	days EMD

### 6.1. Density Estimation

Table 8 presents distance metrics for density estimation distributions. We see that the continuous models outperform the discrete models and that the Continuous RNN is likely preferred, as it has the lowest distances throughout, other than for sequence lengths.

For participation and transition rates, EMD can be approximately interpreted as the expected difference between the real and synthesised rates within a schedule. For example, the minimum EMD of schedule length, of the Continuous CNN, is 0.1. This can be interpreted as an expected error of 0.1 too many or too few activities per schedule. Similarly, the minimum EMD of participation is 0.033. This can be interpreted as an expected error of 3.3% too many or too few of any activity type within a schedule.

For timing, distances can be approximately interpreted as the expected difference, in days, between the real and modelled timings of activities. For example, the minimum difference in activity durations, by the Continuous RNN, is 0.16. This can be interpreted as an expected error in activity duration of 0.016 days, or 23 minutes.

Figures 11 and 12 present both *aggregate* activity frequencies (participations binned at 10-minute intervals) and *disaggregate* activity sequences, for the modelled and target real samples. Synthetic distributions should look like the target real distribution. Notably, we can see that the Discrete CNN has excellent aggregate performance, but is less convincing in disaggregate, for example, introducing additional stay-at-home sequences. The introduction of such sequences is common amongst all the discrete models.

The continuous models reliably generate reasonable-looking sequences, but only the Continuous RNN, with its good timing density estimation, produces a reasonable-looking distribution of aggregate frequencies.

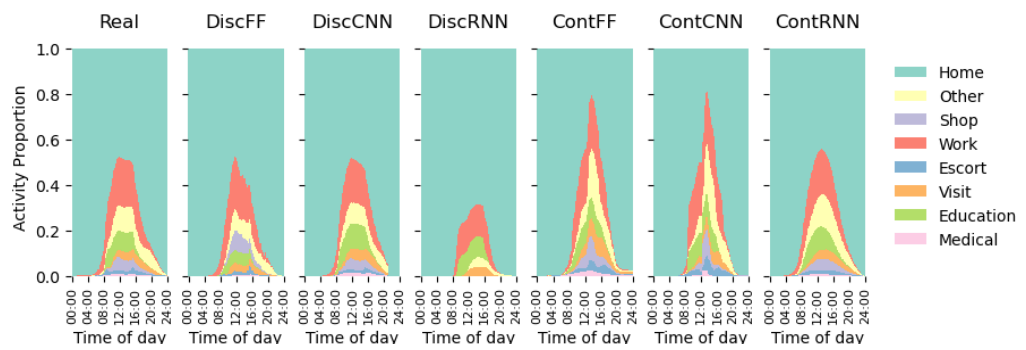


Figure 11: Aggregate Activity Frequencies (10-minute time bins)

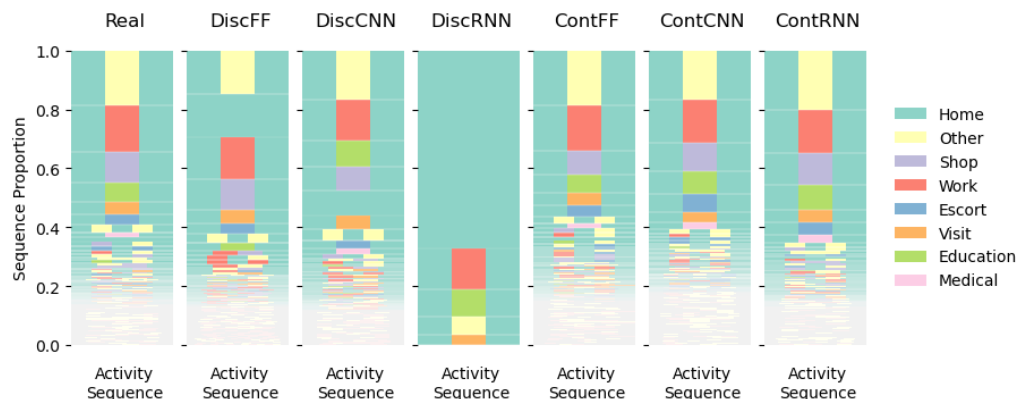


Figure 12: Activity Sequences

Table 9: Sample Quality Evaluations

	Discrete			Continuous			Unit
	FF	CNN	RNN	FF	CNN	RNN	
Not home-based	<b>0.000</b>	<b>0.000</b>	0.050	0.032	0.005	0.001	prob.
Consecutive	<b>0.000</b>	<b>0.000</b>	<b>0.000</b>	0.028	0.025	0.018	prob.
Invalid (combined)	<b>0.000</b>	<b>0.000</b>	0.050	0.057	0.030	0.018	prob.

### 6.2. Sample Quality

Table 9 presents the probabilities that schedules are structurally invalid, either because they are not home-based or they contain consecutive home, work or education activities. The discrete models perform best in general. This is at least partly because they are structurally incapable of generating consecutive activities of the same type and therefore do not generate consecutive home, work or education activities. However they also not generate non-home based schedules, with the exception of the Discrete RNN.

These results should be interpreted carefully, as the real sample has this structure artificially imposed as described in Section 2.5. The observed NTS schedules do contain non-home-based schedules and consecutive home, work or education activities, although rarely. We can alternatively interpret the discrete models as being unable to generate consecutive activities, which could be considered negative. It is perhaps more reasonable to consider this measure of sample quality as a measure of how easily the models can be restricted to comply with some downstream requirement, such as all schedules starting and ending with home activities. In this particular case, the discrete models would be preferable.

The best performing continuous model, the Continuous RNN, produces invalid schedules only 2% of the time, and non-home-based schedules only 0.1% of the time. In a broader modelling framework, any structurally unsuitable schedules would likely be either fixed or rejected and resampled, although this might introduce bias. We choose not to implement such fixing or rejection sampling in this paper to better expose the trade-offs between the models.

### 6.3. Creativity

Table 10 presents the creativity descriptive metrics. Model creativity is considered a combination of homogeneity and conservatism. Homogeneity is the probability that generated schedules are not unique, and conservatism is the probability that generated schedules are found in the training dataset. In both cases, we consider lower as better.

The continuous models show higher creativity than the discrete models. The Continuous RNN, in particular, generates 98% unique and 99% novel schedules. However, this is partly due to the higher temporal precision of the continuous encoding.

## 7. Selected Models Density Estimation

Overall, we find that the Continuous RNN is preferred for most applications. It combines both the best density estimation and the best creativity. It has only minor sample quality issues, for example, only generating 0.1% non-home-based schedules.

Table 10: Creativity Evaluations

	Discrete			Continuous			Unit
	FF	CNN	RNN	FF	CNN	RNN	
Homogeneity	0.468	0.507	0.931	0.153	0.348	<b>0.022</b>	prob.
Conservatism	0.100	0.118	0.351	0.011	<b>0.010</b>	0.012	prob.

The following sections review the density estimation of the Continuous RNN in detail, comparing it to the best-performing discrete model, the Discrete CNN. The following tables present descriptive metrics for distributions using mean density. This is useful for qualitative evaluation but can hide differences between distributions, which are better measured using EMD or visualised in the following figures. As above, all metrics are presented as means (and standard deviations) from five model runs.

### 7.1. Participations

Mean densities of participation rates are compared in Table 11 for the real and synthetic samples from the Discrete CNN and Continuous RNN. Participations measure the number of occurrences, i.e. the rate, of each activity type in every schedule, then use the mean density as a descriptive metric for each sample. This can be interpreted as the expected number of participations in each activity. The Continuous RNN is better than the Discrete CNN at sequence lengths and single activity participation rates. For example, the expected Continuous RNN sequence length is 3.840 activities, close to the real expected length of 3.894.

The comparison of pair participations, which consider joint dependencies within schedules (anywhere within a schedule, not necessarily consecutive), is less clear. However, as per the aggregated results in Table 8 the Continuous RNN is better performing overall (an expected EMD of 0.004 versus 0.011). This is due to the Continuous RNN performing well across all activity combinations, including infrequent ones.

Note that activity pairs create a large number of combinations. For conciseness, we only show the ten most frequent and the ten least frequent. Combinations such as *escort + other* occur in the synthetic samples but not in the real sample. However, we note that whilst these combinations do not occur in the real sample, there is no structural reason why they either could not or should not occur; in other words, they are *sampling zeros* rather than *structural zeros*. Further inspection reveals that these zero-samples are more common in the Discrete CNN sample, although they still occur infrequently.

### 7.2. Transitions

Transition density estimation considers the mean densities of different activity transitions. Transitions are sequences, two, three or four activities long. Called bi-grams, tri-grams and quad-grams respectively. As per Table 8, the Continuous RNN outperforms the Discrete CNN at the aggregated distribution level for all cases.

Table 12 details mean densities of transition rates for the ten most and ten least frequently observed bi-grams, tri-grams and quad-grams. These represent progressively longer sequences of transitions. The mean density of a transition can be interpreted as the expected number of each transition in a schedule. For example, the most common

Table 11: Activity Participation Rates - Mean Densities and EMD

	Real /Target	Discrete CNN			Continuous RNN			Unit
		mean*	std*	EMD	mean*	std*	EMD	
<b>Sequence Length</b>								
sequence length	3.894	3.496	0.073	0.399	3.840	0.062	<b>0.154</b>	length
<b>Participation</b>								
home	2.306	2.088	0.030	0.219	2.264	0.025	<b>0.057</b>	rate
other	0.524	0.442	0.015	0.082	0.489	0.024	<b>0.037</b>	rate
shop	0.291	0.242	0.041	0.057	0.298	0.037	<b>0.036</b>	rate
work	0.256	0.295	0.014	0.040	0.264	0.019	<b>0.016</b>	rate
escort	0.256	0.107	0.029	0.149	0.230	0.050	<b>0.055</b>	rate
visit	0.128	0.157	0.026	0.032	0.146	0.019	<b>0.031</b>	rate
education	0.090	0.114	0.014	<b>0.026</b>	0.115	0.008	<b>0.026</b>	rate
medical	0.043	0.052	0.018	0.016	0.034	0.006	<b>0.009</b>	rate
<b>Pair Participation</b>								
home+home	1.039	0.914	0.012	0.125	1.030	0.010	<b>0.024</b>	rate
other+other	0.086	0.066	0.008	0.021	0.078	0.006	<b>0.009</b>	rate
home+other	0.084	0.065	0.008	0.019	0.076	0.006	<b>0.008</b>	rate
escort+escort	0.075	0.019	0.008	0.056	0.050	0.009	<b>0.025</b>	rate
home+escort	0.072	0.019	0.008	0.054	0.048	0.008	<b>0.024</b>	rate
shop+shop	0.033	0.028	0.012	<b>0.012</b>	0.047	0.016	0.014	rate
home+shop	0.033	0.027	0.012	<b>0.011</b>	0.045	0.015	0.013	rate
visit+visit	0.013	0.015	0.003	<b>0.003</b>	0.011	0.003	<b>0.003</b>	rate
home+visit	0.013	0.015	0.003	<b>0.003</b>	0.011	0.003	<b>0.003</b>	rate
home+work	0.011	0.026	0.005	0.015	0.014	0.003	<b>0.003</b>	rate
...	...	...	...	...	...	...	...	
education+medical	0.000	0.000	0.000	<b>0.000</b>	0.000	0.000	<b>0.000</b>	rate
visit+medical	0.000	0.000	0.000	<b>0.000</b>	0.000	0.000	<b>0.000</b>	rate
education+escort	0.000	0.000	0.000	<b>0.000</b>	0.000	0.000	<b>0.000</b>	rate
education+shop	0.000	0.000	0.000	<b>0.000</b>	0.000	0.000	<b>0.000</b>	rate
education+work	0.000	0.001	0.002	0.001	0.000	0.000	<b>0.000</b>	rate
visit+escort	0.000	0.000	0.000	<b>0.000</b>	0.000	0.000	<b>0.000</b>	rate
medical+escort	0.000	0.000	0.001	<b>0.000</b>	0.000	0.000	<b>0.000</b>	rate
medical+other	0.000	0.000	0.001	<b>0.000</b>	0.000	0.000	<b>0.000</b>	rate
shop+other	0.000	0.001	0.001	<b>0.001</b>	0.001	0.001	<b>0.001</b>	rate
escort+other	0.000	0.001	0.002	0.001	0.000	0.001	<b>0.000</b>	rate

\* mean and standard deviation of descriptive metric

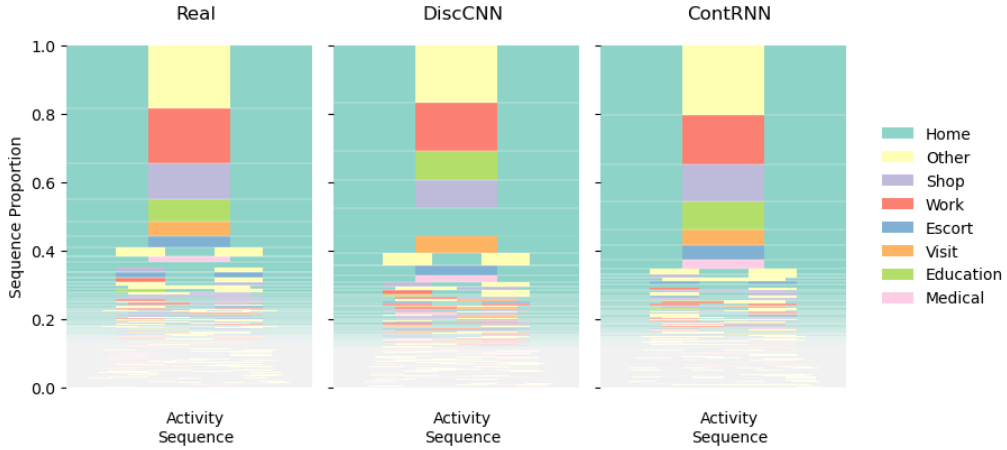


Figure 13: Whole Schedule Sequences

single transition, the bi-gram *home-other* has an average rate of 0.450 in the real sample. This can be interpreted as the expected number of such transitions in a schedule. The synthetic Discrete CNN and Continuous RNN samples have expected *home-other* rates of 0.414 and 0.403, underestimating the mean density of these transitions by only 0.04 of a single transition.

Similarly to participation frequencies, both models generate *zero-samples* (sequences not observed in the real sample), such as *work-medical-visit*. However, we also note that these do not necessarily represent *structural-zeros* and could reasonably be expected to occur.

Figure 13 shows the frequencies of whole schedule activity sequences. Both models maintain the pattern of common shorter sequences and uncommon longer sequences. However, the Discrete CNN introduces a significant increase in *stay-at-home* sequences, from 1.6% in the real sample to 8.2%. Conversely, the Continuous RNN under-generates *stay-at-home* sequences by about 50% (approximately 0.8% of schedules generated by the Continuous RNN are *stay-at-home* sequences).

### 7.3. Timing

Figure 14 compares the distributions of start times, end times and durations for different activities. Figure 15 compares the joint distributions of activity start times and durations. In both cases, the synthetic samples should resemble the target real sample. Notably, the Discrete CNN performs well at escort activity timing, capturing the bi-modal distribution well, but poorly at work activity timing, often generating unrealistically short *work* activities.

Table 13 compares start times and durations for the 20 most common activities. Note that activities are enumerated, such that *home0* denotes the first home activity in a sequence and *home1* the second, and so on. Times (either start times or durations) are measured in days. We use the mean density as the descriptive metric, which we interpret as the expected start time or duration. For example, *work0* has a real expected start

Table 12: Activity Transition Rates - Mean Densities and EMD

	Real /Target	Discrete CNN			Continuous RNN			Unit
		mean*	std*	EMD	mean*	std*	EMD	
<b>2-grams</b>								
home-other	0.450	0.414	0.010	<b>0.042</b>	0.403	0.024	0.048	rate
other-home	0.444	0.408	0.011	<b>0.042</b>	0.394	0.022	0.050	rate
shop-home	0.246	0.225	0.039	0.038	0.228	0.017	<b>0.021</b>	rate
home-work	0.238	0.275	0.022	0.037	0.232	0.014	<b>0.015</b>	rate
work-home	0.227	0.255	0.019	0.029	0.226	0.012	<b>0.011</b>	rate
home-shop	0.221	0.190	0.044	0.049	0.211	0.019	<b>0.016</b>	rate
home-escort	0.198	0.086	0.022	0.112	0.179	0.039	<b>0.043</b>	rate
escort-home	0.190	0.080	0.022	0.110	0.159	0.040	<b>0.051</b>	rate
visit-home	0.102	0.117	0.016	<b>0.020</b>	0.127	0.018	0.029	rate
home-visit	0.095	0.101	0.013	<b>0.012</b>	0.101	0.013	0.013	rate
...	...	...	...	...	...	...	...	
education-med	0.000	0.001	0.001	0.001	0.000	0.000	<b>0.000</b>	rate
med-education	0.000	0.001	0.002	0.001	0.000	0.000	<b>0.000</b>	rate
education-work	0.000	0.017	0.007	0.017	0.001	0.001	<b>0.001</b>	rate
shop-education	0.000	0.002	0.004	0.002	0.001	0.000	<b>0.000</b>	rate
work-education	0.000	0.014	0.004	0.014	0.000	0.000	<b>0.000</b>	rate
<b>3-grams</b>								
home-other-home	0.394	0.361	0.016	<b>0.039</b>	0.327	0.022	0.068	rate
home-work-home	0.214	0.232	0.025	0.026	0.200	0.011	<b>0.015</b>	rate
home-shop-home	0.191	0.163	0.039	0.044	0.163	0.021	<b>0.028</b>	rate
home-escort-home	0.143	0.055	0.015	0.089	0.119	0.030	<b>0.040</b>	rate
home-education-home	0.079	0.070	0.019	0.020	0.088	0.010	<b>0.011</b>	rate
home-visit-home	0.076	0.076	0.008	<b>0.007</b>	0.083	0.010	0.012	rate
other-home-other	0.051	0.055	0.009	0.012	0.040	0.004	<b>0.011</b>	rate
escort-home-escort	0.039	0.007	0.004	0.031	0.025	0.005	<b>0.013</b>	rate
home-med-home	0.031	0.029	0.008	0.006	0.029	0.004	<b>0.004</b>	rate
shop-home-other	0.030	0.018	0.005	0.012	0.020	0.006	<b>0.010</b>	rate
...	...	...	...	...	...	...	...	
med-visit-work	0.000	0.000	0.000	<b>0.000</b>	0.000	0.000	<b>0.000</b>	rate
visit-escort-med	0.000	0.000	0.000	<b>0.000</b>	0.000	0.000	<b>0.000</b>	rate
visit-med-work	0.000	0.000	0.000	<b>0.000</b>	0.000	0.000	<b>0.000</b>	rate
visit-work-med	0.000	0.000	0.000	<b>0.000</b>	0.000	0.000	<b>0.000</b>	rate
work-med-visit	0.000	0.000	0.000	<b>0.000</b>	0.000	0.000	<b>0.000</b>	rate
<b>4-grams</b>								
other-home-other-home	0.123	0.145	0.028	<b>0.040</b>	0.078	0.006	0.045	rate
home-other-home-other	0.122	0.143	0.028	0.040	0.085	0.010	<b>0.037</b>	rate
home-escort-home-escort	0.087	0.018	0.008	0.069	0.054	0.012	<b>0.033</b>	rate
escort-home-escort-home	0.087	0.017	0.008	0.069	0.047	0.008	<b>0.039</b>	rate
shop-home-other-home	0.074	0.046	0.012	<b>0.028</b>	0.044	0.017	0.029	rate
home-shop-home-other	0.061	0.036	0.010	<b>0.024</b>	0.037	0.013	<b>0.024</b>	rate
home-other-home-shop	0.051	0.014	0.005	0.037	0.038	0.005	<b>0.013</b>	rate
other-home-shop-home	0.049	0.012	0.004	0.037	0.030	0.002	<b>0.019</b>	rate
work-home-other-home	0.046	0.042	0.005	<b>0.005</b>	0.030	0.006	0.016	rate
home-work-home-other	0.046	0.041	0.006	<b>0.006</b>	0.031	0.006	0.015	rate
...	...	...	...	...	...	...	...	
work-visit-home-med	0.000	0.000	0.000	<b>0.000</b>	0.000	0.000	<b>0.000</b>	rate
work-visit-med-visit	0.000	0.000	0.000	<b>0.000</b>	0.000	0.000	<b>0.000</b>	rate
work-visit-other-med	0.000	0.000	0.000	<b>0.000</b>	0.000	0.000	<b>0.000</b>	rate
work-visit-other-work	0.000	0.000	0.000	<b>0.000</b>	0.000	0.000	<b>0.000</b>	rate
work-visit-work-med	0.000	0.000	0.000	<b>0.000</b>	0.000	0.000	<b>0.000</b>	rate

\* mean and standard deviation of descriptive metric

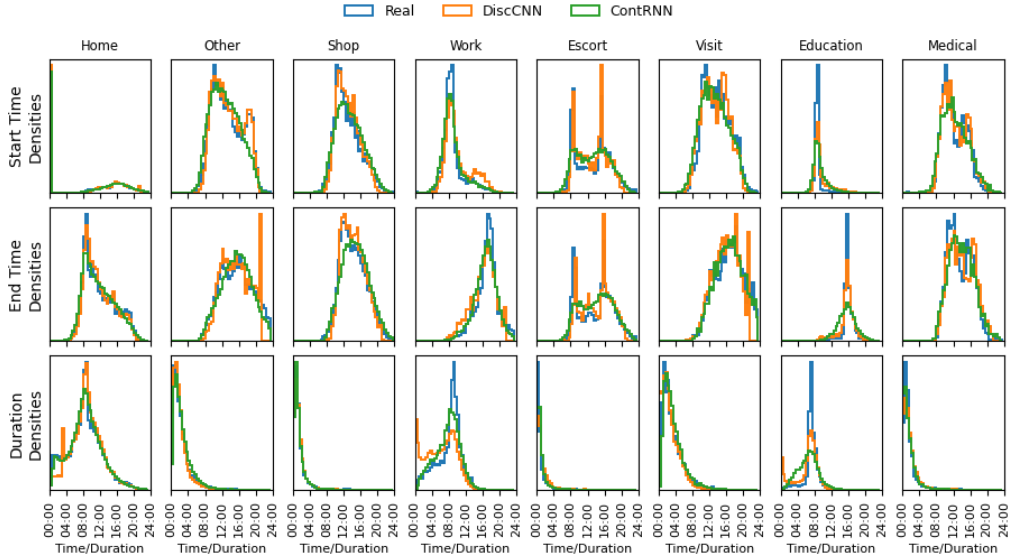


Figure 14: Activity Start Times and Durations

time of 0.365 days (from midnight) and duration of 0.342 days, corresponding to 8:45 and just over 8 hours.

Table 14 shows joint activity start times and durations, and joint consecutive activity durations. Consecutive durations are segmented by the type of the first activity. We use the L1 norm for these two-dimensional distributions, such that descriptions and distances can be interpreted as the sum of times and/or durations. For example, *medical* has the lowest real expected joint start duration of 0.571 days. This can be interpreted as some combination of starting early and or being of short duration. These distributions also capture more subtle patterns, for example, early start times may be associated with long durations and vice versa.

As per Table 8, the Continuous RNN is better performing overall, however from Tables 13 and 14 we observe that the Discrete CNN tends to be better at the timing of short duration activities such as *other*, *shop*, *visit*, and *medical*, but worse at longer duration activities such as *home*, *work*, and *education*.

## 8. Sample Size Scenarios

To evaluate the best performing model, the Continuous RNN, with different quantities of training data, we down-sample the real population by 50%, 25% and 12.5%. With the original real sample, this corresponds to real sample sizes of approximately 60,000, 30,000, 15,000 and 7,500.

For each sample size, we train and evaluate both the base Continuous RNN model and a sub-model. Each sub-model is specifically designed for each sample size. The sub-models, Continuous RNN *Mid*, Continuous RNN *Small* and Continuous RNN *Tiny*

Table 13: Activity Start Times and Durations

	Real /Target	Discrete CNN			Continuous RNN			Unit
		mean*	std*	EMD	mean*	std*	EMD	
<b>Start Times</b>								
home0	0.000	0.000	0.000	<b>0.000</b>	0.000	0.000	<b>0.000</b>	days
home1	0.626	0.635	0.007	0.021	0.640	0.019	<b>0.018</b>	days
other0	0.537	0.539	0.009	<b>0.014</b>	0.521	0.006	0.017	days
home2	0.721	0.756	0.008	0.049	0.746	0.022	<b>0.027</b>	days
shop0	0.530	0.527	0.008	<b>0.017</b>	0.548	0.027	0.024	days
work0	0.365	0.389	0.007	<b>0.025</b>	0.388	0.016	0.028	days
escort0	0.499	0.514	0.013	0.039	0.505	0.014	<b>0.020</b>	days
visit0	0.562	0.553	0.004	<b>0.014</b>	0.573	0.030	0.023	days
education0	0.362	0.401	0.014	0.040	0.381	0.009	<b>0.027</b>	days
other1	0.636	0.668	0.011	0.035	0.614	0.019	<b>0.023</b>	days
escort1	0.627	0.619	0.013	0.036	0.618	0.012	<b>0.021</b>	days
home3	0.758	0.762	0.013	<b>0.028</b>	0.791	0.023	0.034	days
medical0	0.508	0.503	0.016	<b>0.016</b>	0.522	0.017	0.025	days
shop1	0.586	0.620	0.007	0.042	0.590	0.031	<b>0.024</b>	days
other2	0.673	0.672	0.015	0.018	0.664	0.015	<b>0.017</b>	days
escort2	0.662	0.647	0.026	0.031	0.662	0.011	<b>0.014</b>	days
visit1	0.641	0.610	0.020	0.035	0.649	0.019	<b>0.021</b>	days
work1	0.590	0.592	0.006	<b>0.018</b>	0.603	0.020	0.030	days
home4	0.788	0.754	0.036	0.046	0.811	0.021	<b>0.026</b>	days
<b>Durations</b>								
home0	0.456	0.506	0.007	0.050	0.457	0.011	<b>0.013</b>	days
home1	0.281	0.303	0.008	0.026	0.278	0.013	<b>0.013</b>	days
other0	0.092	0.092	0.006	<b>0.008</b>	0.102	0.010	0.013	days
home2	0.219	0.230	0.007	0.033	0.207	0.017	<b>0.018</b>	days
shop0	0.054	0.066	0.008	0.012	0.055	0.003	<b>0.007</b>	days
work0	0.342	0.277	0.006	0.064	0.318	0.009	<b>0.027</b>	days
escort0	0.035	0.050	0.005	0.017	0.042	0.006	<b>0.013</b>	days
visit0	0.128	0.109	0.004	<b>0.019</b>	0.157	0.018	0.029	days
education0	0.300	0.229	0.027	0.072	0.266	0.011	<b>0.046</b>	days
other1	0.073	0.069	0.004	<b>0.008</b>	0.091	0.013	0.021	days
escort1	0.025	0.044	0.003	<b>0.019</b>	0.046	0.002	0.021	days
home3	0.194	0.201	0.009	0.021	0.181	0.018	<b>0.018</b>	days
medical0	0.057	0.068	0.003	<b>0.013</b>	0.085	0.045	0.031	days
shop1	0.041	0.050	0.006	0.013	0.052	0.005	<b>0.012</b>	days
other2	0.059	0.054	0.006	<b>0.008</b>	0.079	0.009	0.022	days
escort2	0.025	0.043	0.007	<b>0.019</b>	0.044	0.004	0.020	days
visit1	0.091	0.069	0.005	<b>0.022</b>	0.119	0.020	0.031	days
work1	0.139	0.082	0.009	0.057	0.169	0.023	<b>0.032</b>	days
home4	0.167	0.200	0.026	0.044	0.169	0.014	<b>0.015</b>	days
escort3	0.022	0.040	0.017	0.023	0.040	0.004	<b>0.018</b>	days

\* mean and standard deviation of descriptive metric

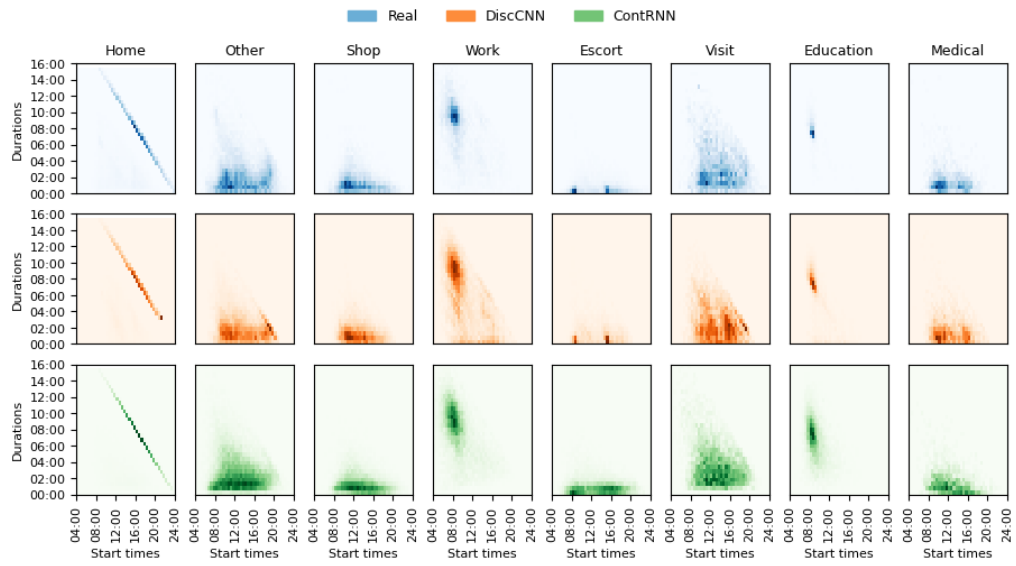


Figure 15: Joint Activity Start Times, End Times and Durations

Table 14: Joint Activity Start Times and Durations

	Real /Target	Discrete CNN			Continuous RNN			Unit
		mean*	std*	EMD	mean*	std*	EMD	
<b>Joint Start Durations</b>								
home	0.722	0.741	0.002	0.074	0.722	0.006	<b>0.023</b>	days
other	0.651	0.652	0.007	<b>0.023</b>	0.641	0.014	0.034	days
shop	0.594	0.606	0.006	<b>0.027</b>	0.613	0.029	0.031	days
work	0.712	0.670	0.006	0.115	0.710	0.011	<b>0.057</b>	days
escort	0.584	0.588	0.010	0.054	0.584	0.008	<b>0.033</b>	days
visit	0.699	0.667	0.007	<b>0.036</b>	0.734	0.040	0.049	days
education	0.667	0.630	0.012	0.153	0.649	0.009	<b>0.074</b>	days
medical	0.571	0.582	0.015	<b>0.025</b>	0.609	0.041	0.055	days
<b>Joint Consecutive Durations</b>								
home	0.507	0.548	0.014	0.055	0.525	0.017	<b>0.031</b>	days
other	0.319	0.335	0.007	<b>0.028</b>	0.332	0.016	0.032	days
shop	0.330	0.352	0.020	0.038	0.305	0.022	<b>0.037</b>	days
work	0.543	0.477	0.017	0.096	0.513	0.021	<b>0.051</b>	days
escort	0.248	0.305	0.024	0.060	0.262	0.018	<b>0.031</b>	days
visit	0.325	0.317	0.011	<b>0.041</b>	0.359	0.024	0.055	days
education	0.569	0.425	0.042	0.150	0.537	0.013	<b>0.075</b>	days
medical	0.331	0.310	0.040	<b>0.056</b>	0.421	0.034	0.098	days

\* mean and standard deviation of descriptive metric

Table 15: Continuous RNN Sub-Model Hyper-Parameters

Model	Block Size (NxS)	Latent Size	Learning Rate	Batch Size	$\beta$	$\alpha$	Drop Out
ContRNN (Base)	4x256	6	0.001	1024	0.01	200	0.1
ContRNN Mid	2x256	6	0.002	1024	0.005	200	0.1
ContRNN Small	2x128	6	0.004	1024	0.0025	200	0.1
ContRNN Tiny	2x64	6	0.008	1024	0.00125	200	0.1

Table 16: Sample Size Scenarios Evaluation Summary

Model:	Continuous RNN								Unit
	Base	Base	Mid	Base	Small	Base	Tiny		
<b>Sample Size:</b>									
100%	50%			25%		12.5%			
<b>Density Estimation</b>									
Participations	0.064	0.085	0.098	0.147	0.186	0.214	0.449	rate	EMD
Transitions	0.004	0.006	0.005	0.036	0.012	0.055	0.053	rate	EMD
Timing	0.025	0.030	0.035	0.060	0.057	0.089	0.121	days	EMD
<b>Sample Quality</b>									
Invalid	0.018	0.030	0.019	0.071	0.055	0.279	0.144	prob.	
<b>Creativity</b>									
Homogenous	0.022	0.009	0.007	0.086	0.015	0.070	0.190	prob.	
Conservative	0.012	0.007	0.006	0.006	0.003	0.004	0.003	prob.	

have alternative hyperparameters specifically recalibrated for each of the sample sizes as per Table 15.

Table 16 summarises results from this experiment. We see a clear trend in worsening density estimation and sample quality as the sample size decreases, with a particularly steep drop-off at 12.5%. The steep drop in performance at around 7,500 schedules likely represents a hard limit to the deep generative approach.

We show that using smaller models specifically calibrated for each sample size partly mitigates the impact of less data. By using the Continuous RNN *Mid* with 30,000 schedules, performance is comparable to the full sample and base model. This is true for all evaluation metrics other than participation density estimation, which is generally improved with larger models. We expect that larger sample sizes will result in better results, although with diminishing returns.

## 9. COVID-19 Scenario

Finally, we consider applying the Continuous RNN model to a behavioural change scenario. We extract schedules from the NTS travel diaries as per Section 2.5, but create two new real samples for 2019 and 2020. We chose these samples as we expect a change in schedule distributions due to COVID-19 from 2019 to 2020. We name these samples *Real 2019* and *Real 2020*. Both samples have 23,452 schedules, significantly less than the

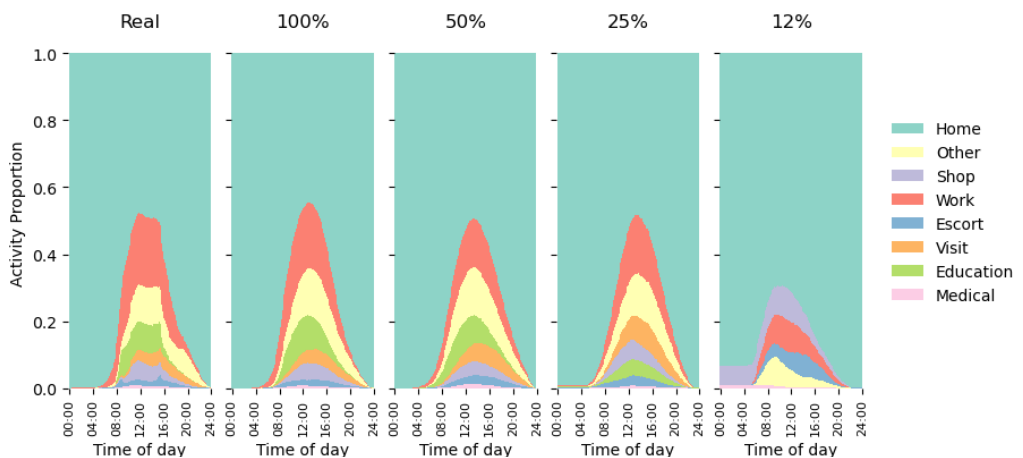


Figure 16: Sample Sizes Scenarios: Aggregate Activity Frequencies (10 minute time bins)

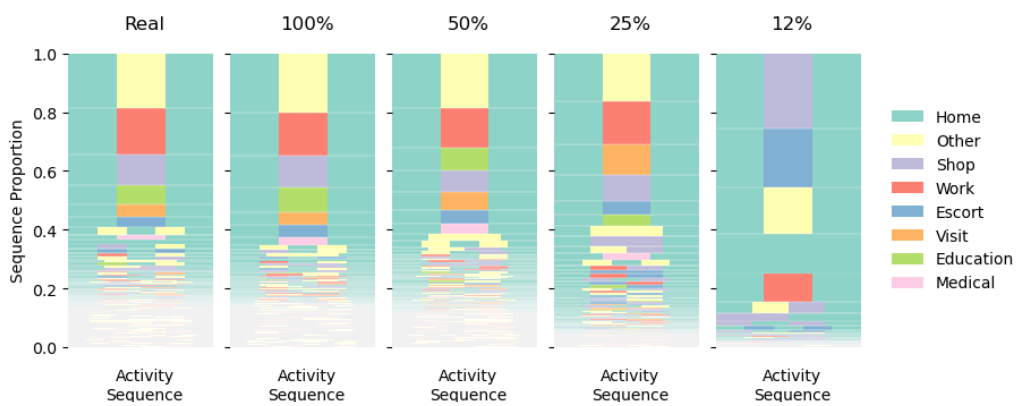


Figure 17: Sample Sizes Scenarios: Activity Sequences

base 2023 sample, so we train a Continuous RNN *Mid* (Table 15) for each sample year, then generate synthetic samples from both. We name these samples *Synthetic 2019* and *Synthetic 2020*.

Table 17 summarises mean densities for the real and synthetic 2019 and 2020 scenario distributions, which can be interpreted as expected values for the various distributions shown. We consider whether the changes in schedules from 2019 and 2020 observed in the real samples are also present in the synthetic samples. To consider real and synthetic changes between 2019 and 2020, we use the difference in mean densities rather than EMD so that the direction of change can additionally be considered.

Both synthetic samples (2019 and 2020) show lower levels of participation than their respective real samples. However, the change from 2019 to 2020 is well represented in the synthetic populations. Most notably, from 2019 to 2020, the real expected sequence length drops from 3.887 to 3.717 (-0.171). Although the synthetic samples both underestimate sequence length, they show a similar drop from 3.700 to 3.527 (-0.173). Single and pair participations show a similar pattern, suggesting that although the models appear biased to lower activity participation, this bias is consistent across scenarios, such that the behaviour change is captured.

Transitions are extremely similar between the real samples, so they are not considered. For timing estimation, the models capture both real sample distributions well and therefore also show similar changes between 2019 and 2020. For example, there is a shift to activities starting 0.016 days (23 minutes) earlier in real samples, and 0.015 days (22 minutes) earlier in the synthetic samples.

This experiment suggests that the approach can capture differences between samples of schedules. Specifically, we show that the model design has not been overfit to the original 2023 scenario and can be re-trained to capture new patterns of schedules, such as for 2019 and 2020. However, we also show that the reported differences between synthetic and real samples, particularly for participations, are comparable to changes observed between 2019 and 2020 due to COVID-19.

## 10. Results Discussion

We find that encoding choice, i.e. discrete or continuous, dominates model selection. We strongly recommend the use of the continuous encoding in most cases. If a discrete encoding is being used, we suggest the use of a CNN-based architecture as per the Discrete CNN.

The best-performing model, the Continuous RNN, is composed of both the continuous schedule encoding and an RNN architecture, both of which introduce additional complexity compared to the Discrete CNN. This complexity is broadly due to treating scheduling as both a categorical problem (for activity types) and a continuous problem (for activity durations). Specifically, the continuous encoding requires an additional hyperparameter  $\alpha$ . However, we find that all the models are reasonably insensitive to hyperparameter selection, such that models can be quickly optimised with grid search or similar.

Hyperparameter tuning is also facilitated by fast model training times. Table 18 shows model sizes and expected run times based on an NVIDIA RTX A5000 GPU. The Continuous RNN is trained in only 4.2 minutes and generates approximately 60,000

Table 17: COVID Scenario Mean Densities

	Real			Synthetic*			Unit
	2019	2020	Diff	2019	2020	Diff	
<b>Participations</b>							
sequence length	3.887	3.717	-0.171	3.700	3.527	-0.173	rate
participation rate	0.486	0.465	-0.021	0.462	0.441	-0.022	rate
pair participation rate	0.041	0.039	-0.002	0.037	0.036	-0.002	rate
<b>Transitions</b>							
2-gram	0.049	0.046	-0.002	0.049	0.050	0.001	rate
3-gram	0.006	0.006	0.000	0.007	0.008	0.001	rate
4-gram	0.002	0.003	0.000	0.003	0.005	0.001	rate
<b>Timing</b>							
start times	0.428	0.412	-0.016	0.427	0.413	-0.015	days
start-durations	0.690	0.686	-0.004	0.700	0.698	-0.001	days
durations	0.257	0.269	0.012	0.270	0.284	0.013	days
joint-durations	0.434	0.445	0.011	0.460	0.470	0.010	days

\* mean of mean density from 5 model runs

Table 18: Model Sizes and Run Times

Model	Trainable Params (millions)	Memory (Mb)	Training Time (min)	Generation Time (sec)
DicsFF	116.2	467.8	4.3	1.4
DiscCNN	8.5	33.8	4.8	1.2
DiscRNN	16.9	67.6	95.8	8.9
ContFF	30.2	120.7	2.1	0.7
ContCNN	0.2	1.0	2.4	0.5
ContRNN	4.3	17.0	4.2	1.4

schedules in only 1.4 seconds. A full synthetic sample for the UK (68.3 million) could be generated in less than 30 seconds. This speed makes model and hyperparameter search cheap, moving the bottleneck in model development to the user and the evaluation tools. We provide Caveat<sup>5</sup> to allow reproduction of results and enable extensive model and hyperparameter exploration.

Experiments with smaller data samples in Section 8 show that more data leads to better results. Smaller models can be used for smaller datasets, but the deep generative approach becomes unviable at around 7,500 schedules or fewer. Our COVID-19 scenario in Section 9 shows that the Continuous RNN model design and hyperparameter specification can capture differences between samples with different patterns of schedules. However, this scenario also suggests that the expected differences in participation rates may be non-trivial.

## 11. Conclusions

We demonstrate the synthesis of large, diverse samples of realistic activity schedules with a deep generative approach based on a VAE architecture. Our work shows that a deep generative modelling approach can approximate a complex human behavioural system. Our generative approach makes rapid and diverse synthesis, upsampling or anonymisation of observed activity schedules feasible. Such samples can then be used for applied models and simulations in the transport, energy and epidemiology domains.

We use a comprehensive evaluation framework to compare alternative schedule encodings and model designs. We show that a novel continuous schedule encoding is preferable to a standard discrete encoding, although it adds complexity to model design and specification.

Our best-performing Continuous RNN model achieves both aggregate and disaggregate realism. This model combines continuous schedule encoding and a recurrent structure within the VAE encoder and decoder architectures. However, this model exhibits some poor sample quality, for example, generating non-home-based schedules 0.1% of the time.

Depending on the application, structural zero samples might need to be removed from synthetic samples and new schedules generated, or otherwise fixed, which might introduce bias. More generally, compared to traditional approaches, which are easier to constrain, this inability to impose specific structures on generated schedules should be considered a disadvantage. However, in many cases, it is likely acceptable given the gain in speed, simplicity and realistic distribution. The choice of a discrete encoded model, which has some imposed structure, could also be considered for some specific applications.

All models can generate millions of sequences in seconds. They have minor stochastics and are not overly sensitive to hyperparameters. This makes them a practical choice for human activity modelling frameworks using synthetic schedules.

### 11.1. Further Research

For this work, we focus on a deep generative VAE architecture, which we find to have adequate capacity for this task. We note that alternative generative approaches are available and could be formally compared.

---

<sup>5</sup><https://github.com/big-ucl/caveat>

We find some trade-offs between the Discrete CNN and Continuous RNN models for the generation of times for short versus long activities. This might be purely the result of biases within the chosen encodings and architectures, but might also reflect different choice-making processes for different activities. Further work should look to remove this trade-off. For example, by adding time of day context to the Continuous RNN architecture.

The application of the current work is limited to where activity schedule generation is not conditional. For traditional transport modelling frameworks, non-conditioned generation is only adequate if schedules are assumed static. This is sometimes the case when developing short-term scenarios or if the model's focus is on subsequent transport supply simulation scenarios. However, in most transport demand modelling frameworks, conditionality is required, typically for changing socio-demographics and accessibility. Further work will therefore look to add conditionality to the generative process.

Further work should also look to increase the complexity of schedule generation. For example, extending to multiple days, incorporating additional activity types, trips, and additional attributes such as location or travel mode choice. We share Caveat<sup>6</sup> to provide a framework for further model development and evaluation.

## 12. Acknowledgements

This work was supported by the Engineering and Physical Sciences Research Council (EPSRC) [grant numbers EP/T517793/1 and EP/W524335/1].

## References

Akiba, T., Sano, S., Yanase, T., Ohta, T., Koyama, M., 2019. Optuna: A next-generation hyperparameter optimization framework, in: Proceedings of the 25th ACM SIGKDD International Conference on Knowledge Discovery and Data Mining.

Arentze, T.A., Timmermans, H.J., 2004. A learning-based transportation oriented simulation system. *Transportation Research Part B: Methodological* 38, 613–633. doi:<https://doi.org/10.1016/j.trb.2002.10.001>.

Auld, J., Mohammadian, A., 2009. Framework for the development of the agent-based dynamic activity planning and travel scheduling (adaps) model. *Transportation Letters* 1, 245–255.

Badu-Marfo, G., Farooq, B., Patterson, Z., 2020. A differentially private multi-output deep generative networks approach for activity diary synthesis. [arXiv:2012.14574](https://arxiv.org/abs/2012.14574).

Borysov, S.S., Rich, J., Pereira, F.C., 2019. Scalable Population Synthesis with Deep Generative Modeling. *Transportation Research Part C: Emerging Technologies* 106, 73–97. doi:[10.1016/j.trc.2019.07.006](https://doi.org/10.1016/j.trc.2019.07.006), [arXiv:1808.06910](https://arxiv.org/abs/1808.06910).

Bowman, S.R., Vilnis, L., Vinyals, O., Dai, A.M., Józefowicz, R., Bengio, S., 2015. Generating sentences from a continuous space. *CoRR* abs/1511.06349.

Bradley, M., Bowman, J.L., Griesenbeck, B., 2010. Sacsim: An applied activity-based model system with fine-level spatial and temporal resolution. *Journal of Choice Modelling* 3, 5–31.

Drchal, J., Čertický, M., Jakob, M., 2016. VALFRAM: Validation Framework for Activity-Based Models. *Journal of Artificial Societies and Social Simulation* 19, 5.

Goodfellow, I., Pouget-Abadie, J., Mirza, M., Xu, B., Warde-Farley, D., Ozair, S., Courville, A., Bengio, Y., 2014. Generative adversarial nets, in: Ghahramani, Z., Welling, M., Cortes, C., Lawrence, N., Weinberger, K. (Eds.), *Advances in Neural Information Processing Systems*, Curran Associates, Inc.

---

<sup>6</sup><https://github.com/big-ucl/caveat>

Gregor, K., Danihelka, I., Graves, A., Rezende, D., Wierstra, D., 2015. Draw: A recurrent neural network for image generation, in: Bach, F., Blei, D. (Eds.), Proceedings of the 32nd International Conference on Machine Learning, PMLR, Lille, France. pp. 1462–1471.

Hafezi, M.H., Daisy, N.S., Millward, H., Liu, L., 2021. Ensemble learning activity scheduler for activity based travel demand models. *Transportation Research Part C: Emerging Technologies* 123, 102972. URL: <https://www.sciencedirect.com/science/article/pii/S0968090X21000097>, doi:<https://doi.org/10.1016/j.trc.2021.102972>.

Ho, J., Jain, A., Abbeel, P., 2020. Denoising diffusion probabilistic models, in: Larochelle, H., Ranzato, M., Hadsell, R., Balcan, M., Lin, H. (Eds.), Advances in Neural Information Processing Systems, Curran Associates, Inc.. pp. 6840–6851.

Hochreiter, S., Schmidhuber, J., 1997. Long Short-Term Memory. *Neural Computation* 9, 1735–1780. doi:[10.1162/neco.1997.9.8.1735](https://doi.org/10.1162/neco.1997.9.8.1735).

Horni, A., Nagel, K., Axhausen, K. (Eds.), 2016. Multi-Agent Transport Simulation MATSim. Ubiquity Press, London. doi:[10.5334/baw](https://doi.org/10.5334/baw).

Khan, N.A., Habib, M.A., 2023. Microsimulation of activity generation, activity scheduling and shared travel choices within an activity-based travel demand modelling system. *Travel Behaviour and Society* 32, 100590. doi:<https://doi.org/10.1016/j.tbs.2023.100590>.

Kim, E.J., Bansal, P., 2023. A deep generative model for feasible and diverse population synthesis. *Transportation Research Part C: Emerging Technologies* 148, 104053. doi:[10.1016/j.trc.2023.104053](https://doi.org/10.1016/j.trc.2023.104053).

Kim, E.J., Kim, D.K., Sohn, K., 2022. Imputing qualitative attributes for trip chains extracted from smart card data using a conditional generative adversarial network. *Transportation Research Part C: Emerging Technologies* 137, 103616. doi:[10.1016/j.trc.2022.103616](https://doi.org/10.1016/j.trc.2022.103616).

Kingma, D.P., Welling, M., 2013. Auto-Encoding Variational Bayes. doi:[10.48550/arXiv.1312.6114](https://doi.org/10.48550/arXiv.1312.6114), [arXiv:1312.6114](https://arxiv.org/abs/1312.6114).

Kingma, D.P., Welling, M., 2019. An introduction to variational autoencoders. *Foundations and Trends® in Machine Learning* 12, 307–392. URL: <http://dx.doi.org/10.1561/2200000056>, doi:[10.1561/2200000056](https://doi.org/10.1561/2200000056).

Koushik, A., Manoj, M., Nezamuddin, N., Prathosh, AP., 2023. Activity Schedule Modeling Using Machine Learning. *Transportation Research Record* 2677, 1–23. doi:[10.1177/03611981231155426](https://doi.org/10.1177/03611981231155426).

Liao, X., Jiang, Q., He, B.Y., Liu, Y., Kuai, C., Ma, J., 2024. Deep activity model: A generative approach for human mobility pattern synthesis. URL: <https://arxiv.org/abs/2405.17468>, [arXiv:2405.17468](https://arxiv.org/abs/2405.17468).

Liu, F., Janssens, D., Cui, J., Wets, G., Cools, M., 2015. Characterizing activity sequences using profile hidden markov models. *Expert Systems with Applications* 42, 5705–5722. doi:<https://doi.org/10.1016/j.eswa.2015.02.057>.

Lucas, T., Shmelkov, K., Alahari, K., Schmid, C., Verbeek, J., 2019. Adaptive density estimation for generative models, in: Wallach, H., Larochelle, H., Beygelzimer, A., d'Alché-Buc, F., Fox, E., Garnett, R. (Eds.), Advances in Neural Information Processing Systems, Curran Associates, Inc. URL: [https://proceedings.neurips.cc/paper\\_files/paper/2019/file/959ab9a0695c467e7caf75431a872e5c-Paper.pdf](https://proceedings.neurips.cc/paper_files/paper/2019/file/959ab9a0695c467e7caf75431a872e5c-Paper.pdf).

Manser, P., Haering, T., Hillel, T., Pougala, J., Krueger, R., Bierlaire, M., 2021. Resolving temporal scheduling conflicts in activity-based modelling. URL: <https://transp-or.epfl.ch/documents/technicalReports/ManserEtAl2021.pdf>.

Miller, E.J., Roorda, M.J., 2003. Prototype model of household activity-travel scheduling. *Transportation Research Record* 1831, 114–121.

Miller, E.J., Roorda, M.J., Carrasco, J.A., 2005. A tour-based model of travel mode choice. *Transportation* 32, 399–422.

Naeem, M.F., Oh, S.J., Uh, Y., Choi, Y., Yoo, J., 2020. Reliable fidelity and diversity metrics for generative models, in: III, H.D., Singh, A. (Eds.), Proceedings of the 37th International Conference on Machine Learning, PMLR. pp. 7176–7185. URL: <https://proceedings.mlr.press/v119/naeem20a.html>.

Nayak, S., Pandit, D., 2023. A joint and simultaneous prediction framework of weekday and weekend daily-activity travel pattern using conditional dependency networks. *Travel Behaviour and Society* 32, 100595. URL: <https://www.sciencedirect.com/science/article/pii/S2214367X23000467>, doi:<https://doi.org/10.1016/j.tbs.2023.100595>.

Ord, A.V.D., Kalchbrenner, N., Espeholt, L., Kavukcuoglu, K., Vinyals, O., Graves, A., 2016. Conditional image generation with pixelcnn decoders. *ArXiv* abs/1606.05328.

Pendyala, R.M., Kitamura, R., Kikuchi, A., Yamamoto, T., Fujii, S., 2005. Florida activity mobility simulator: overview and preliminary validation results. *Transportation Research Record* 1921, 123–130.

Pougalas, J., Hillel, T., Bierlaire, M., 2023. Oasis: Optimisation-based activity scheduling with integrated simultaneous choice dimensions. *Transportation Research Part C: Emerging Technologies* 155, 104291. doi:<https://doi.org/10.1016/j.trc.2023.104291>.

Rezende, D., Mohamed, S., 2015. Variational inference with normalizing flows, in: Bach, F., Blei, D. (Eds.), *Proceedings of the 32nd International Conference on Machine Learning*, PMLR, Lille, France. pp. 1530–1538.

Rezende, D.J., Mohamed, S., Wierstra, D., 2014. Stochastic backpropagation and approximate inference in deep generative models, in: *International conference on machine learning*, PMLR. pp. 1278–1286.

Roberts, A., Engel, J., Raffel, C., Hawthorne, C., Eck, D., 2018. A hierarchical latent vector model for learning long-term structure in music, in: Dy, J., Krause, A. (Eds.), *Proceedings of the 35th International Conference on Machine Learning*, PMLR. pp. 4364–4373.

Sajjadi, M.S.M., Bachem, O., Lucic, M., Bousquet, O., Gelly, S., 2018. Assessing generative models via precision and recall, in: Bengio, S., Wallach, H., Larochelle, H., Grauman, K., Cesa-Bianchi, N., Garnett, R. (Eds.), *Advances in Neural Information Processing Systems*, Curran Associates, Inc. URL: [https://proceedings.neurips.cc/paper\\_files/paper/2018/file/f7696a9b362ac5a51c3dc8f098b73923-Paper.pdf](https://proceedings.neurips.cc/paper_files/paper/2018/file/f7696a9b362ac5a51c3dc8f098b73923-Paper.pdf).

Sener, I.N., Bhat, C.R., Copperman, R., Srinivasan, S., Guo, J.Y., Pinjari, A., Eluru, N., 2006. Activity-based travel-demand analysis for metropolitan areas in Texas: CEMDAP models, framework, software architecture and application results. Technical Report. Midwest Regional University Transportation Center.

Shone, F., Chatzioannou, T., Pickering, B., Kozlowska, K., Fitzmaurice, M., 2024. PAM: Population Activity Modeler. *Journal of Open Source Software* 9, 6097. doi:[10.21105/joss.06097](https://doi.org/10.21105/joss.06097).

Theis, L., van den Oord, A., Bethge, M., 2016. A note on the evaluation of generative models, in: Bengio, Y., LeCun, Y. (Eds.), *4th International Conference on Learning Representations, ICLR 2016, San Juan, Puerto Rico, May 2-4, 2016, Conference Track Proceedings*. URL: <http://arxiv.org/abs/1511.01844>.

Vaswani, A., Shazeer, N., Parmar, N., Uszkoreit, J., Jones, L., Gomez, A.N., Kaiser, L.u., Polosukhin, I., 2017. Attention is all you need, in: Guyon, I., Luxburg, U.V., Bengio, S., Wallach, H., Fergus, R., Vishwanathan, S., Garnett, R. (Eds.), *Advances in Neural Information Processing Systems*, Curran Associates, Inc.